Chemosphere 296 (2022) 133974

Contents lists available at ScienceDirect

Chemosphere

journal homepage: www.elsevier.com/locate/chemosphere

New analytical strategies Amplified with 2D carbon nanomaterials for electrochemical sensing of food pollutants in water and soils sources

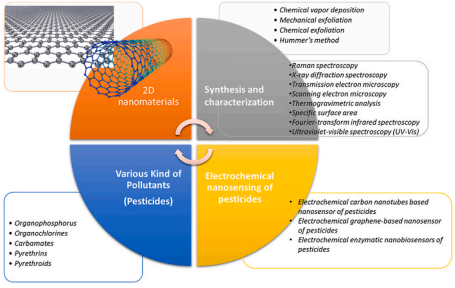
Goksu Ozcelikay [a], Leyla Karadurmus [a,b], Selva Bilge [c], Ali Sınağ [c], Sibel A. Ozkan [a,*]

[a] Ankara University, Faculty of Pharmacy, Department of Analytical Chemistry, 06560, Ankara, Turkey
[b] Adıyaman University, Faculty of Pharmacy, Department of Analytical Chemistry, Adıyaman, Turkey
[c] Ankara University, Faculty of Science, Department of Chemistry, 06100, Ankara, Turkey

HIGHLIGHTS

- Synthesis and characterization of 2D-carbon nanomaterials.
- Overview of pesticides that threaten life in drugs, lake water, and soil sources.
- Application of graphene and CNT integrated nanosensor and enzymatic nanobiosensors.

GRAPHICAL ABSTRACT



ARTICLE INFO

Handling Editor: Derek Muir

Keywords:
2D-carbon nanomaterials
Graphene
Carbon nanotubes
Pesticides
Enzyme nanobiosensors

ABSTRACT

Pharmaceutical and food pollutants have threatened global health. Pharmacotherapy has left a positive impression in the field of health and life of people and animals. However, the many unresolved problems brought along with residues of pharmaceuticals in the environmental and food. Consumption of the world's freshwater resources, toxic chemicals, air pollution, plastic waste directly affects water and soil resources. Pesticides have a wide role in pollutants. Therefore, the determination of pesticides is significant to eliminate their negative effects on living things. Nowadays, there are many analytical methods available. However, new analysis methods are still being researched due to certain limitations of traditional methods. Electrochemical sensors have drawn attention because of their superior properties, such as short analysis time, affordability, high sensitivity, and selectivity. The development of new analytical strategies for assessing risks from pharmaceutical to food pollutants in water and soil sources is important for the measurement of different pollutants.

Moreover, the 2D-carbon nanomaterials used in the development of electrochemical sensors are widely utilized to enlarge the surface area, increase porosity, and make easy immobilization. Graphene (graphene derivations) and carbon nanotubes integrated nanosensors are widely used for the determination of pesticides. 2D-carbon nanomaterials can be tailored according to the purpose of the study. The characterization and synthesis methods of 2D-carbon nanomaterials are widely explained. Furthermore, enzyme nanobiosensors, especially Acetylcholinesterase (AChE), are widely used to determine pesticides. The three main topics are focused on in this review: 2D-carbon nanomaterials, pesticides that threaten life, and the application of 2D-carbon nanomaterials-based electrochemical sensors. The various developed 2D-carbon nanomaterials-based

* Corresponding author.
E-mail address: ozkan@pharmacy.ankara.edu.tr (S.A. Ozkan).

https://doi.org/10.1016/j.chemosphere.2022.133974
Received 18 October 2021; Received in revised form 13 January 2022; Accepted 11 February 2022
Available online 15 February 2022
0045-6535/© 2022 Elsevier Ltd. All rights reserved.

electrochemical sensors were applied in pharmaceutical forms, fruits, tap/lake water, beverages, and soils sources. This work aims to indicate the recently published paper related to pesticide analysis and highlight the importance of 2D-nanomaterials on sensors.

1. Introduction

Contamination of chemicals from the environment is a global food safety problem that poses a serious threat to human health. Monitoring contamination levels, enacting control measures, including remediation, and considering impacts are vital to providing safer food globally. These chemicals are metals/metalloids, polycyclic aromatic hydrocarbons (PAHs), persistent organic pollutants (POPs), perfluorinated compounds (PFCs), pharmaceutical and personal care products (PPCPs), radioactive elements, electronic waste, plastics, and nanoparticles. Some of these occur naturally in the environment, while others are produced from anthropogenic sources. They can contaminate our crops, livestock and seafood, and drinking water and have adverse effects on our health (Nag et al., 2018; Pedrero et al., 2017; Thompson and Darwish, 2019; Wang et al., 2016).

Chemical contamination is a global food safety problem. Many potentially toxic substances in the environment can contaminate food consumed by humans. They contain inorganic and organic substances and can come from a wide variety of sources. One of the most important environmental pollutants is pesticides. The Food and Drug Administration (FDA) is responsible for enforcing tolerances by the Environmental Protection Agency (EPA) for amounts of pesticide residues that can legally remain in foods. The analytical methods utilized by EPA and FDA to define pesticide residues on foods are found in the Pesticide Analytical Manual (PAM). FDA publishes the PAM as a storage of the analytical methods utilized in FDA laboratories to investigate food for pesticide residues for regulatory goals. Identifying and determining environmental and food pollutants are important research topics in analytical chemistry, as they pose a serious threat to human health. Focusing on this issue, various methodologies involving the use of two-dimensional carbon nanomaterials electrochemical platforms have recently been reported in the literature. This review describes current electrochemical strategies in which the design of two-dimensional carbon nanomaterials plays a key role in the determination of pollutants in food and environmental samples. The modification aspects of two-dimensional carbon nanomaterials for electrochemical sensors, their synthesis and characterization, the electrochemical platform design, and the advantages that two-dimensional carbon nanomaterials provide in the analysis of target analytes are critically analyzed discussed. This review covers electrochemical sensor applications of the technique for isolating pollutants from food and the environmental samples published recently (Nag et al., 2018; Pedrero et al., 2017; Thompson and Darwish, 2019; Wang et al., 2016).

2D-carbon nanomaterials used in the development of electrochemical sensors are one of the most widely utilized to enlarge the surface area, increase porosity, and make easy immobilization. This review focused on using the 2D carbon nanomaterials for electrochemical sensing of pharmaceutical and food pollutants in water and soils sources. In this context, the current study presents the advances in 2D carbon nanomaterial-based electrochemical sensors developed for water and soils sources. The importance of this area and current advances in the analysis have been extensively emphasized (Le et al., 2021; Vasseghian et al., 2022).

2. Modification aspects of two-dimensional carbon nanomaterials for electrochemical sensors

Carbon is a vital element with allotropic diversity due to its versatile bonding ability. Carbon is known as the constituent of living organisms, making it indispensable for scientific and technological developments. A simple carbon atom has four valence electrons, two in the 2s orbital and two in the 2p orbital. While the carbon atom forms bonds with the other carbon atoms around it, it bonds by sp hybridization by increasing the existing electron in the 2s orbital to the vacant 2p orbital (Wu et al., 2010). There are three types of sp hybridization: sp, sp2, and sp3 hybridizations. Carbon atoms that make sp2 and sp3 hybridizations can form graphene and diamond derivatives by forming three and four bonds with neighboring carbon atoms. Today, two-dimensional carbon nanomaterials are considered the most popular material for electrochemical sensor applications. Particularly, graphene-based nanomaterials are becoming the focus of attention for electrochemical pesticide determination. Graphene, graphene oxide, reduced graphene oxide, and carbon nanowalls are the primary functional materials that form two-dimensional carbon materials (Li and Mu, 2019). The unique properties of two-dimensional nanomaterials, such as high chemical stability, good electrical conductivity, high surface area, and high electron transfer, make them preferable for electrochemical sensor applications (Huang et al., 2011). Two-dimensional carbon materials are essential as they are the basis for understanding the electronic properties in 0D, 1D, and 3D structured allotropes. In this respect, elucidation of the properties, synthesis methods, and characterization of 2D carbon nanomaterials are crucial (Nasrollahzadeh et al., 2021).

2.1. Graphene

Graphene, the most functional and vital material of the two-dimensional carbon nanomaterial class, has a benzene-like honeycomb skeleton (Allen et al., 2010). In addition, graphene is formed by the arrangement of many carbon atoms, which make sp2 hybridization. Graphene has low magnetic properties due to long-term coulomb interactions and short-term electron-electron interactions (Castro Neto et al., 2009). However, the flexibility of 2D graphene leads to the improvement of its electronic properties. In addition, this material is a highly conductive material both thermally and electrically due to its moisture-resistant structure and high electron mobility. For this reason, graphene will always be an indispensable material for battery, supercapacitor, and sensor applications (Liu et al., 2012).

Especially in electrochemical sensors, the large surface area helps the desired biomolecules to be transported in the solution medium. Furthermore, graphene provides effective interaction between the analyte molecule and the electrode surface due to its high surface area and porosity (Castro Neto et al., 2009).

2.2. Graphene oxides

Graphene oxide (GO) is an unusual 2D material composed of oxygen-containing functional groups. Due to the presence of surface functional groups, this material exhibits a very different electronic character compared to pristine graphene (Liu et al., 2012). These characteristics make them indispensable for electrochemical sensor applications. Focusing on the basal plane of graphene oxide, it has been proven that it mainly consists of epoxy (–O–) and hydroxyl (–OH) groups. The structure of GO sheets is highly suitable for heteroatom doping or polymer bonding applications, making them easy to use as electrode modification materials. These applications increase the electrical conductivity of the materials in the solution media (Nag et al., 2018).

2.3. Reduce graphene oxides

Although GO disperses very well in an aqueous solution due to its

oxygenated functional groups, this feature leads to a significant disadvantage because it causes a very significant decrease in layer conductivity (Guex et al., 2017). Therefore, GO is reduced in the presence of various reducing agents, and its electrical conductivity properties are improved (Agharkar et al., 2014). The increased carbon-oxygen ratio in the GO layers theoretically provides higher electrical conductivity. However, significant differences occur in electrical conductivity values when different reduction protocols and agents are applied in the GO reduction process (Peres et al., 2006).

2.4. Carbon nanowalls

Carbon nanowalls (CNWs) consist of vertically positioned graphene sheets. In addition, CNWs show two-dimensional walls with large surface areas and sharp edges. The thickness of CNWs ranges from 1 to 10 nm (Mostofizadeh et al., 2011). In the last decade, it has been possible to synthesize well-aligned two-dimensional CNWs on various substrate surfaces using improved chemical vapor deposition methods. CNWs have unique physical properties due to the functionality of their scaffolds; therefore, they are promising in sensor applications (Wu et al., 2002).

3. Synthesis and characterization of graphene and its derivatives

3.1. Synthesis of graphene and its derivatives

3.1.1. Chemical vapor deposition

The chemical vapor deposition (CVD) technique is essential in which multilayer film-like materials are obtained using metal substrates based on high-temperature pyrolysis of carbon-based gases. This technique is the focus of researchers in terms of the development and improvement of graphene materials. Many different transition metals such as Co, Ni, Fe, Ru, Rh, Ir Pd, Pt, and Au are preferred to synthesize graphene through the CVD technique. Although CVD graphene synthesis has shown rapid developments in the past ten years, it has gained a much more functional dimension. Researchers show that it is possible to synthesize polycrystalline graphene with very high quality and large surface area according to its substrate. The adhesion force between graphene and metal substrate is an essential factor determining graphene's electronic character (Whitener and Sheehan, 2014).

3.1.2. Mechanical exfoliation

Mechanical exfoliation techniques (micromechanical cleavage, sonication, ball milling, fluid dynamics) vary widely. The mechanical exfoliation technique is based on treating graphite with a top-bottom approach. The achievement of this technique depends on obtaining graphene by peeling off the graphite layer by layer. Another important aspect is to overcome the van der Waals attraction forces between graphene layers. To separate these layers from each other, it is necessary to resort to micromechanical splitting with Scotch tape. In addition, a situation that should be considered in this technique is the fragmentation effect. The force produced by the exfoliation technique can also break up large graphite particles, facilitating exfoliation (Yi and Shen, 2015).

3.1.3. Chemical exfoliation

The best-known technique adopted for the large-scale synthesis of graphene sheets is the chemical exfoliation technique. The exfoliation of graphite is due to the mixture of $(NH_4)_2S_2O_8$, H_2SO_4, and fuming H_2SO_4. Also, recently, the exfoliation performance of graphite has been enhanced by using a binary mixture containing CH_3CO_3H and H_2SO_4. The resulting graphene sheets are perfectly dispersed in aqueous media (Yusuf et al., 2019).

3.1.4. Hummer's method

There are different Hummer methods, including modified and improved hummer methods. The basis of the Hummer method is based on the reduction of graphite after oxidation in the presence of agents such as $NaNO_3$ and $KMnO_4$. However, $NaNO_3$, an oxidative agent, causes the emission of toxic and harmful gases such as NO_X. For this reason, the use of $NaNO_3$ is eliminated in the modified hummer method, and a mixture of H_2SO_4 and H_3PO_4 is used (Nag et al., 2018).

3.2. Characterization of graphene and its derivatives

Various analysis methods applied for graphene and its derivatives are briefly summarized.

3.2.1. Raman spectroscopy

Raman spectroscopy is an important technique that provides the structural characterization of graphene. It is a characterization technique that provides information about the vibrational states of the atoms that make up the material. Raman shifts are also a beneficial technique for investigating the electronic structure of carbon-derived materials (Yusuf et al., 2019). Thanks to this technique, the electronic properties of graphene, the density of defects in its skeleton, and the simple structure of its layers can be elucidated. The common feature of graphene and all graphene-based materials is that they have three characteristic peaks (G band at 1580 cm^{-1}, D band at 1350 cm^{-1}, and 2D band at 2680 cm^{-1}) in Raman spectroscopy (Malard et al., 2009). The G band is caused by in-plane vibrations of atoms from sp2 hybridization, which is the most critical feature of graphite-based materials. The 2D band is evidence of the existence of electronic tapes that multilayer graphene has. The D band is related to the positioning of the sp2 atoms in the honeycomb structure that makes up the graphene structure. The ratio of the D and G band intensities gives information about the disorder in the graphene structure (Childres et al., 2013).

3.2.2. X-ray diffraction spectroscopy

X-ray diffraction (XRD) patterns for single-layer graphene are helpful in determining the structure, but they are not sufficient on their own. In general, pure graphite (pristine) peaks in the region of $2\theta = 26.68^{\circ}$. However, it shifts to a 2θ lower angle value (13.98°) after graphite oxidation due to oxygen-containing functional groups in the structure and water retention in the formed layers (Yusuf et al., 2019).

3.2.3. X-ray photoelectron spectroscopy

X-ray photoelectron (XPS) spectroscopy is frequently used to determine the chemical surface properties of graphene and graphene-derived 2D materials. N atom is added to the structure of graphene during the oxidation and reduction processes, so the peak at 400.6 eV is assigned to N-C_{sp3}. The O1s peak in the XPS spectrum is estimated to be from the O═C═OH or C–O groups. On the other hand, the C1s peak of graphene is evidence of the existence of three different functional groups (C–C, C–OH, C═O) (Yusuf et al., 2019).

3.2.4. Transmission electron microscopy

While taking transmission electron microscopy (TEM) images of graphene and its derivatives materials, they are generally operated in the voltage range of 200–300 kV, which causes instability in the structure. To eliminate of this disadvantage, lower voltage ranges should be preferred. Transmission electron microscopy helps visualize the surface morphology of single-layer graphene. Although TEM analysis is advantageous for confirming the thickness of single-layer graphene, it is more accurate to supplement it with atomic force microscopy data. In addition, one of the methods to be followed to determine the layer number of graphene is to take high-resolution TEM images by shifting the incidence angles between the electron beam and graphene from many different regions.

3.2.5. Scanning electron microscopy

Scanning electron microscopy (SEM) is used to investigate the

surface properties of graphene, such as porosity and irregularity (Bachmatiuk et al., 2015). Determination of pore size is essential for the use of graphene in electrochemical sensor applications. Because the pore size distribution is indicative of the adsorption of organic and inorganic molecules on graphene, it is critical in elucidating the ion transfer mechanism that occurs on the material surface, especially in electrochemical measurements performed in a solution medium (Yusuf et al., 2019).

3.2.6. Thermogravimetric analysis

The thermogravimetric analysis (TGA) method is used as a powerful analytical tool for qualitative and quantitative analysis of graphene-like materials. TGA results show that mass loss is observed due to the evaporation of water molecules in the nitrogen atmosphere and below 100°. rGO is more thermally stable because there are more oxygenated functional groups than GO.

3.2.7. Specific surface area

One of the best ways to distinguish graphene and its derivatives from each other is to determine their specific surface area. Each graphene-like material has its surface area value, as well as electrical conductivity and d-space. Therefore, it is crucial to establish a relationship between high surface area and interlayer distance (d-spacing) and ID/IG. In contrast, the high surface area is expected to lead to high electrical conductivity due to improving the conductivity character. Therefore, the three critical parameters that shape the electrical conductivity character of graphene-derived materials are the specific surface area, d range, and ID/IG, respectively (Mohan et al., 2020).

3.2.8. Fourier-transform infrared spectroscopy

Fourier-transform infrared spectroscopy (FTIR) measures the absorption/transmittance of light and converts it into a function of wavelength, thus helping to identify the functional groups present in the structure. Especially since graphene and its derivatives contain different types of oxygenated groups, FTIR plays a critical role in identifying these groups. Furthermore, these functional groups are important in determining the electrical conductivity and the behavior (hydrophobic/hydrophilic) of the material in aqueous media. In general, in the FTIR spectrum obtained for GO, the vibration at 3000- 3700 cm^{-1} indicate the hydroxyl groups, the vibration at 1750-1850 cm^{-1} of the carbonyl groups, the vibration at 1650-1750 cm^{-1} of the carboxy groups, and vibration at 1280–1320/800-900 cm^{-1} are evidence of the presence of epoxy groups (Ţucureanu et al., 2016).

3.2.9. Ultraviolet–visible spectroscopy (UV–Vis)

UV–Vis is the preferred technique to determine the optical absorption character of GO and its derivatives. Nanostructured graphene sheets form an adsorption peak at 265 nm, often evidence of graphitic structure (excitation of π-plasmon). Therefore, the UV–Vis absorption spectrum is often preferred for identification purposes such as FTIR because it is possible to observe the two characteristic peaks of GO with this technique. The first of these peaks is at 231 nm, which corresponds to the π - π * transitions indicating the presence of aromatic C═C bonds, and the second is the shoulder at ~300 nm, which is attributed to the n- π * transitions of the C═O bonds (Zhang et al., 2019c).

4. Various kind of pollutants in food and environmental samples

Identifying environmental and food pollutants is an important research topic in analytical chemistry as they cause serious harm to human health. In this regard, many publications have been reported in the literature in recent years. In this section, contaminants are described in food and environmental samples. Environmental pollutants are chemicals that cause damage to the environment, often accidently or intentionally, as a result of human activities. These pollutants released into the environment can enter the food chain and harm human health. Many different environmental pollutants have been detected in foods (Nag et al., 2018; Pedrero et al., 2017; Wang et al., 2016). These range from "ionic" species such as metals and perchlorate to organic substances, including "persistent organic pollutants" or POPs (Thompson and Darwish, 2019).

There are many polluting and potentially toxic substances in the environment. These include inorganic and organic substances and can come from a wide variety of sources. The source of the pollutants can be the environment. These are metals such as lead and mercury, dioxins, and polychlorinated biphenyls (PCBs). Likewise, drugs used in both humans and animals can contaminate waterways and pose a health risk to consumers. Toxicity may be related to the route of exposure and dose, and personal characteristics such as age and health status may affect an individual's susceptibility. Agricultural use of pesticides can cause food contamination. In the next section, pesticides are explained in detail (Mahmood and Malik, 2014; Thompson and Darwish, 2019).

4.1. Overview of pesticides in food and environmental analysis

The use of plant protection products is essential and helps secure global food supplies but can leave pesticide residues in our food chain. It causes environmental risks and ecological damage due to the toxic effects of pesticides on various living organisms. Insecticides are the most toxic group of pesticides, followed by herbicides, acaricides, and fungicides. Where pesticides, especially insecticides, are routinely used, adverse effects on beneficial organisms are greater. In addition, the endocrine-disrupting effects of some pesticides are much discussed. Pesticide resistance is increasing due to the improper use of compounds. Although many pesticides can be analyzed using conventional analytical techniques, many more cannot be analyzed or can only be analyzed with insufficient sensitivity (Zacharia and Tano, 2011). Therefore, the development of simple, rapid, and selective methods for pesticide residue detection is important for sensitive and accurate monitoring of these residues. Most pesticide residue analyzes were performed using gas chromatography and liquid chromatography techniques (Tadeo, 2008; Tadeo et al., 2019). However, traditional procedures for sample preparation prior to chromatographic analysis are expensive, time-consuming, requiring technicians and expensive equipment. New and improved methods and technologies for the analysis of pesticide residues have become very important in recent years (Nunes et al., 1998).

Pesticides are basically divided into four main groups: organophosphorus, organochlorines, carbamates and pyrethrins, and pyrethroids. They contain both synthetic and plant-based pesticides. In addition, some inorganic compounds are also used as pesticides. Pesticides are produced to destroy, and because their mode of influence is not species-specific, they can destroy or harm organisms other than usual pests, including humans. The World Health Organization estimates millions of pesticide poisoning cases and thousands of deaths each year, mainly in developing countries. Pesticides cause the production of reactive oxygen species that reduce antioxidant levels and defenses against oxidative damage in the cellular system. Due to the imbalance, lipids, proteins, and nucleic acids are targeted, and cellular signaling pathways are influenced (Zacharia and Tano, 2011). Oxidative stress and reactive oxygen species lead to long-term health problems such as carcinogenesis, neurodegeneration, cardiovascular, respiratory, renal, endocrine, and reproductive problems. When pesticides disrupt the oxidative balance, they pave the way for these diseases and homeostasis (Tadeo, 2008; Tadeo et al., 2019).

5. Electrochemical nanosensing of pesticides in food and environmental samples

Electrochemical sensors are mainly chemical sensors that transform into a measurable signal. The analytical signal is obtained by chemical reactions between analyte and recognition transducers. These chemical

sensors are called biosensors, in which the analytical signal is the output of biochemical reactions. The large amount and abuse usage of chemicals and pesticides has threatened living health. It has become one of the most serious problems in the world. Therefore, the fast and simple monitoring of pesticides by analytical methods in water and soil sources is very important. For the past years, several biosensors have been developed to determine pollutants residue, such as electrochemical, optical, and mechanical detection methods (Ba Hashwan et al., 2020). Electrochemical biosensors are useful analytical tools for pollutants detection due to their remarkable properties, including the affordable, user-friendly, portable, and rapid signal.

The importance of nanotechnology in applying electrochemical biosensors is widely known due to enhancing the performance of biosensors and facilitating the immobilization of the bioreceptors. Novel functional nanomaterials, including carbon-based nanomaterials (carbon nanotubes, graphene, and its derivatives), various metal nanoparticles, magnetic nanoparticles, and polymers, are the key components of electrochemical biosensors (Zeng et al., 2016). Electrochemical nano-biosensors with device miniaturization and high sensitivity and specificity bring a new perspective to sense pharmaceutical and food pollutants in water and soils sources.

5.1. Electrochemical carbon nanotubes based nanosensor of pesticides

Carbon nanotubes (CNTs) are widely used as nanomaterials for biosensor applications because of their wide surface areas, specific physical properties, one or more layers, adjustable lengths, and affordable prices. Single-walled carbon nanotubes (SWCNTs) and multi-walled carbon nanotubes (MWCNTs) are valuable candidates to accelerate electron transfer between the electroactive analyte and the electrode surface. Moreover, CNTs can be functionalized with carboxyl or amino groups or form combinations with other materials such as metal nanoparticles, polymers, and ionic liquids to generate additional electrocatalytic sites and increase sensitivity. In the following sections, we illustrate the applications of CNT-based nanobiosensor to analyze pesticides, shown in Table 1.

Santanos Caetano K. et al. described a sensitive electrochemical biosensor for methyl parathion, constructed by MWCNT/zirconia/carbon paste electrode (CPE) [3]. First, MWCNT was dispersed into an ammonium stearate aqueous solution by using the sol-gel method. Then, zirconium *n*-propoxide and acetylacetone were added to the dispersion solution. The MWCNT/zirconia form was kept at ambient conditions. The composite of MWCNT/zirconia and mineral water are homogenously mixed to make the CPE paste. Then, the paste was put in the hole of the CPE. Carbon nanotube provided an enhancement in the signal and a large surface area for pesticides. The ultra-low limit of detection (LOD) as 9 nM was observed for the pesticide sensor. The linear range of the pesticide in MWCNT/zirconia/CPE was defined within 19.9–176.8 μM.

The electrochemical biosensor incorporating ELP-OPH/BSA/TiO_2/c-MWCNTs based as a sensing platform was developed to enhance methyl parathion and parathion (Bao et al., 2016). TiO_2NFs were further used to enrich organophosphates in the nanocomposite due to their strong affinity with a phosphoric group in OPs, while c-MWCNTs were used to enhance the electron transfer. The LOD of the sensor was recorded as 12 nM, and 10 nM for methyl parathion and parathion, respectively, and the linear range is found as up to 36.4 μM.

An electrochemical sensing platform was fabricated with the integration of MWCNTs and $CoFe_2O_4$NPs with an ionic liquid to detect fenitrothion in fruits. IL@CoFe2O4NPs@MWCNTs is an effective GCE modifier due to their ionic conductivity, excellent stability, and biocompatibility. The recorded LOD for the sensor was 0.0135 μM, and the defined linear range was observed from 0.02 to 1600 μM(Kilele et al., 2021).

Another electrochemical sensor was developed with hybrid ferrocene-thiophene modified by carbon nanotube (FT@CNT) to determine parathion and chlorantraniliprole pesticides in tomatoes, apples, and soil samples. The modification agent is prepared the carbon nanotube with thiophene-ferrocene moieties via Click chemistry. This improvement in analytical performance of the electrochemical sensor provided LOD of 5.3 nM and 8.1 nM in the range of 0.02–6.50 μM and 0.01–7.00 μM for parathion and chlorantraniliprole, respectively (Tümay et al., 2021).

5.2. The electrochemical graphene-based nanosensor of pesticides

The research group of A.Geim and K.Novoselov discovered graphene in 2004 (Geim, 2012). The structure of graphene is a two-dimensional nanosheet. Nowadays, graphene and its derivatives (e.g., graphene oxide and reduced graphene oxide) have attracted considerable scientific and technological interest because of its unique physicochemical properties. In the following sections, we provide a broad snapshot of the applications of graphene-based nanobiosensor to analyze pesticides, illustrated in Table 2. Compared with Graphene, the derivatives of it, like graphene oxide (GO) and reduced graphene oxide (rGO), have drawn more attention in the fabrication of biosensors. The main reason is that the derivatives have been given functional groups during chemical oxidation and reduction steps in the preparation process (Zeng et al., 2016).

Akilarasan M. et al. (Akilarasan et al., 2021) conducted a study on electrochemical sensors based on a modified glassy carbon electrode (GCE) with GO and the perovskite $SrTiO_3$. The nanocomposite is synthesized with a hydrothermal approach. GO@$SrTiO_3$-NC/GCE could allow the detection of organochlorine pesticides in the range of 0.01–1.47 μM and 1.47–434.4 μM in river water and soil samples. The LODs for organochlorine pesticide 2,4,6-trichlorophenol was 3.21 nM.

The detection of organophosphorus pesticide (OPS) has garnered growing interest in river water, fruit and vegetable samples. A sensing platform of molecularly imprinted polypyrrole nanotubes (MIPNs) was established for the sensitive and selective detection of Glyphosate (Ding et al., 2021). As seen in Fig. 1a, A 3D printed SPE holder with the ink and MIPNs was used as the working electrode. SEM of MIPNs is given in Fig. 1b. The proposed MIPNs ultimately possessed great features, such as a highly portable and suitable for real-time detection. A standard curve was obtained in the wide range of 2.5–50 $ngmL^{-1}$ for Glyphosate with a remarkably low LOD of 1.94 $ngmL^{-1}$. In addition, MIPNs sensors exhibit good stability, anti-interference abilities, and reproducibility.

Tao T.'s research group pioneered the application of the graphene electrochemical transistor (GECT) using zirconia/reduced graphene oxide (ZrO_2/rGO) nanocomposites (Tao et al., 2021). The electrochemical sensor was designed with ZrO_2/rGO on the gate and the high carrier mobility of graphene in the channel. The developed nanosensor was used to determine methyl parathion with a linear concentration range of 10 $pgmL^{-1}$-10 μgmL^{-1} with LOD of 10 $pgmL^{-1}$.

Zhang C. et al. reported that the disposable electrochemical sensor was fabricated for analysis of cyhexatin (Zhang et al., 2019a). MIP and the synergistic effects of carbon nanomaterials were utilized for enhancing the signal. MIP/AuNPs/ERGO-SPCE is used as a transducer followed by the electropolymerization of *o*-aminothiophenol. Under the optimal condition, the LOD and linear range were found 0.20 $ngmL^{-1}$ and 1–500 $ngmL^{-1}$, respectively. The reproducibility of the response was examined by analysis of the cyhexatin (100 ng mL^{-1}) using independent determinations. The MIP/AuNPs/ERGO-SPCE have acceptable reproducibility with a relative standard deviation of 2.8%.

Zuo Y. et al. demonstrate an electrochemical 2D carbon nanosensor with Pt nanoparticles/MoS_2/graphene nanocomposite to show excellent catalytic activity and great electrochemical signal enhancement towards binaphthol oxidation (Zuo et al., 2020). DPV was successfully conducted in a wide sensing range of 0.4–40 μM for binaphthol measurements with a LOD of 0.07 μM. In addition, an accurate binaphthol concentration is detected in taps water. The authors referred that the developed biosensor is also applied in pharmaceutical industries.

B: Biochar; BDDGR: graphene-modified boron-doped diamond

Table 1
The applications of CNT-based nanobiosensor to analyze pesticides.

Analyte	Method	Enzyme electrode	Linear range	LOD	Recovery	Applications	Reference
Paraoxon	DPV	Nafion/M-Cell/CNT@AAIL/GCE	10–800 fM 0.8–5 pM	3 fM	97.5–104.0%	Tap Water Spinach Juice	Han et al. (2018)
Paraoxon	SWV	CuNCs@BSA- SWCNT/GCE	50–500 nM 0.5–35 μM	12.8 nM	93–104%	River Water Waste Water Well Water	Bagheri et al. (2017)
Methyl Parathion Parathion	Amperometric	ELP-OPH/BSA/TiO_2NFs/c-MWCNTs nanocomposite	0.1–20 μM	12 nM 10 nM	94.6–106.73%	Water Sample	Bao et al. (2016)
Methyl Parathion	Amperometric	MPDE/QD/Cys/AuNPs/MWCNT/GCE	5.0–200 $ngmL^{-1}$ 200-1000 $ngmL^{-1}$	1 $ngmL^{-1}$	96.0–101.3%	Garlic Samples	Du et al. (2010a)
Paraoxon	Amperometric	CS-cMWCNT-HA/BSA/GCE	5–80 μM	0.10 μM	98.4–101.2%	Tap Water	Stoytcheva et al. (2018)
Carbaryl	SWV	MWCNT/CoPc film/GCE	0.33–6.61 μM	5.46 nM	91.9–97.6%	Polluted River Water Sample	Moraes et al. (2009)
Glyphosate Ampa	ECL	nano-ZnO-MWCNT/SPE	1–10 μM 10–100 μM	300 nM 3 μM	92%	0.1 M Phosphate Buffer (Ph 6.9)	Habekost (2017)
Paraquat	DPV	CNT/Nafion/SPCE	0.54–4.30 μM	0.17 μM	82–106%	Natural Water Samples	Chuntib et al. (2017)
Methyl Parathion	DPV	f-SWCNT–ß-CD/GCE	0.002–0.02lμgmL^{-1} 0.02–17.5l μgmL^{-1}	0.4 $ngmL^{-1}$	92.4–107.1%	Onion Sample Lettuce Sample Rape Sample Spinach Sample	Yao et al. (2014)
Diazinon	DPV EIS	VS_2QDs-GNP/cMWCNTs/aptamer/GCE	5×10^{-14}-1x10^{-8} M 1×10^{-14}-1x10^{-8} M	1.1×10^{-14} M 2.0×10^{-15} M	97.0–107.0%	Human Serum Sample River Water Sample Soil Sample Apple Sample Lettuce Sample	Khosropour et al. (2020)
Thiocholine	Amperometric	CoPc-SWCNT/SPE	0.077–0.45 mM	0.038 mM	–	Real Sample	Jubete et al. (2011)
Demeton-S	Amperometric	MWCNT/SPE	Up to 85 μM	1 μM	–	Lake Water Sample	Joshi et al. (2006)
Paraoxon	Amperometric	MWCNT/SPE	Up to 6.9 nM	0.5 nM	90%	Real Water Sample	Joshi et al. (2005)
Physostigmine	DPV	Cu-SWCNT-Pc 3D/GCE	0.1–4.8 μM	53 nM	98.03–104.2%	Orange Juice Sample Peach Juice Sample	Şenocak et al. (2021)
Methyl Parathion	DPV	SWCNT-SubPc-Pc/GCE	2.5 nM-3.75 $\times 10^{-8}$ M	1.78 nM	102.4–104.0%	Orange Juice Sample Cherry Juice Sample	Köksoy et al. (2021)
Dicapthon	DPV	Au NPs@c-MWCNTs/GCE	0-2400 μgL^{-1}	0.009 μgL^{-1}	94.2–97.4%	Cabbage Sample	(Wang et al., 2021a)
Dichlorvos	DPV	Au@MWCNTs/GCE	1–120 μM	5 nM	90.75–97.5%	Leaf Lettuce Sample	(Chen et al., 2021a)
Methyl Parathion	DPV	MWCNT/zirconia/CPE	19.9×10^{-6}-176.8×10^{-6} M	9.0×10^{-9} M	102–113%	Soybean Extract Sample	Caetano et al. (2020)
Methyl Parathion	DPV	CNTs/GCE	1×10^{-7}-3.4×10^{-5} M	3.3×10^{-8} M	86.0–114%	Juice Sample	Michelle et al. (2020)
Methyl Parathion	LSV	h-CNT-μPs/Nafion/GCE	0.3–20.0 μM 20.0–150.0 μM	0.092 μM	96.6–102% 95.5–101.6%	Tomato Sample Cabbage Sample	Yao et al. (2020)
Paraoxon	DPV	CNT/IMZ/GCE	1.2–16 μM	120 nM	88.90–96.79%	Orange Juice Sample	de Oliveira et al. (2020)
Fenitrothion	CV	CNT/GCE	0.54–6.84 μM	0.090 μM	96%	Pistachio Extract Sample	Soltani-Sarvestani et al. (2020)
Nitenpyram	DPV	HCNT/CNH/GCE	20–2000 nM	4 nM	93.4–112.7%,	Corn Sample River Water Sample	(Wang et al., 2020b)
Carbendazim	DPV	CNTs-$MAS_{4.8}$/GCE	0.1–2.0 μM	0.04 μM	90%	Spring Water Sample Commercial Pesticide Sample	Fozing Mekeuo et al. (2021)
Carbendazim	DPV	functionalized and non-functionalized MWCNT electrode	5–200 μM	1.6 μM	92–99%,	Mineral Water Sample Orange Juice Sample	Oliveira et al. (2021)
Parathion Chlorantraniliprole	DPV	FT@CNT/GCE	0.02–6.50 μM 0.01–7.00 μM	5.3 nM 8.1 nM	97.2–104.6%	Apple Sample Soil Sample	Tümay et al. (2021)
Fluometuron	DPV	FePc/MWCNTPE	0.4–15 mgL^{-1}	69.8 μgL^{-1}	96.0%	Tap Water Sample Commercial Herbicide Formulations	Demir et al. (2021)
Fenitrothion	DPV	IL@$CoFe_2O_4$NPs@MWCNTs/GCE	0.02–160 μM		93.8–103.2%		Kilele et al. (2021)

(*continued on next page*)

Table 1 (*continued*)

Analyte	Method	Enzyme electrode	Linear range	LOD	Recovery	Applications	Reference
				0.0135 μM		Orange Sample Grape Sample	
Chlorpyrifos	DPV	CNTs-NH_2/AgNPs-N-F-MoS_2/GCE	5×10^{-8}–10^{-4} mgmL^{-1}	1 pgmL^{-1}	94.6–104.2%	Fruit Sample	Song et al. (2018)
Monocrotophos			10^{-10}–10^{-6} mgmL^{-1}	0.05 mgmL^{-1}			
Sulfentrazone	SWV	MWCNT/SPE	1–25 μM	0.8 μM	98.67–99.0%	Soy Milk Sample Groundwater Sample	Silva et al. (2019)
Tetracycline	EIS	aptamer/MWCNTs-CS/IDAM	10^{-9}-10^{-3} M	1×10^{-9} M	96.7–105.3%	Milk Sample	Hou et al. (2017)
MCPA	CV	PANI-β-CD/fMWCNT/GCE	10–100 μM	0.99 μM	99.5–102%	Phosphate Buffer (Ph 6.0)	Rahemi et al. (2012)
			10–60 μM	–		River Water	
Paraquat	SWV	MWCNTs-DHP/GCE	5×10^{-8}–1.5×10^{-6} M	1×10^{-8} M	95%	Natural Water Sample	Garcia et al. (2013)
	DPV		2×10^{-7}–1.7×10^{-6} M	2.6×10^{-8} M			
Paraoxon-Ethyl	amperometric	MWCNTs-CS/AuNPs/SPE	0.01–10 μgL^{-1} 10-100 μgL^{-1}	0.03 μgL^{-1}	104%	Spinach Sample	Hua et al. (2019)
Acetamiprid	EIS	Au/MWCNT-rGONR/SPE	5×10^{-14}-1x10^{-5} M	1.7×10^{-14} M	96.0–106.6%	Water Sample	Fei et al. (2015)
Dichlorvos	Amperometric	ChOx/PBCB/MWCNT/GCE	2.5–60 nM	1.6 nM	99.7–102.2%	Orange Juice	da Silva et al. (2019)

AAIL: Amino acid ionic liquid; AgNPs-N-F-MoS_2: nitrogen-fluorine co-doped monolayer 2D MoS_2 nanosheet with Ag nanoparticles; BSA: Bovine Serum Albumin; CNH: Carbon nanohorn; CNT: Carbon nanotube; CoPc: Cobalt phthalocyanine; CPE: Carbon paste electrode; CS: Chitsosan; CV: Cyclic voltammetry; Cys: Cysteine; DPV: Differential pulse voltammetry; DHP: dihexadecylhydrogenphosphate; ECL: Electrochemiluminescence; EIS: Electrochemical Impedance Spectroscopy; ELP: Elastin; FePc: iron (III) phthalocyanine; FT: ferrocene-thiophene; GCE: Glassy carbon electrode; GNP: Graphene nanoplate; GO: Graphene oxide; HA: Hydroxyapatite; HCNT: hydroxylated multiwall carbon nanotubes; h-CNT-μPs: Honeycomb CNT-microparticles; IDAM: interdigital array micro-electrode; IL: Ionic liquid; IMT: Imidazole; LSV: Linear sweep voltammetry; MAS: maleic anhydride modified (MAS) *Ayous sawdust*; M-Cell: Mineralized organophosphate hydrolase fused cell; MPDE: Methyl parathion degrading enzyme; MWCNT: Multi walled carbon nanotube; MWCNTPE: multi-walled carbon nanotube paste electrode; NC: Nanocomposite; OPH: Organophosphate; PANI: polyaniline; PBCB: poly(brilliant cresyl blue); Pc-3D: Three dimensional porous hybrid material; rGONR: reduced graphene oxide nanoribbon; SPE: Screen printed electrode; β-CD: Beta cyclodextrin; SubPc-Pc: Subphthalocyanine; SWCNT: Single walled carbon nanotube; SWV: Square wave voltammetry; TiO_2NFs: Titanium dioxide nanofibers; VS_2QDs: Vanadium disulfide quantum dots.

electrode; ChOx: Choline oxidase; CRGO: Chemically reduced graphene oxide; $Dy_2Sn_2O_7$: dysprosium stannate nanoplatelets; ERGO: electrochemically-reduced graphene oxide; Fc-TED: ferrocene containing dendrimer; FeVO: iron vanadium oxide nanoparticles; FTO: fluorine doped tin oxide; g-C_3N_4: Graphitic carbon nitride; GG: graphenized graphite; GN-AuNRs: graphene-AuNRs nanocomposite; GNPs: graphene nanoplatelet; GNR: graphene nanoribbons nanocomposite; GO: Graphene oxide; GQD: Graphene quantum dot; GR: Graphene; ITO: indium tin oxide; MIP: Molecularly imprinted polymer; MIPNs: Molecularly imprinted polypyrrole nanotubes; MNP: magnetite nanoparticles; N-CMK-5: N-doped carbon nanopipe-arrayed mesoporous carbon; N-HG: Nitrogen-doped holey graphene; P3MT/NGE: Poly (3-methylthiophene)/nitrogen doped graphene; PA6/PPy: polyamide 6/polypyrrole; PDDA: poly (diallyldimethyl ammonium); PEI: polyethylenimine; PGE: pencil graphite electrode; PPY-g-NGE: Polypyrrole-grafted nitrogen-doped graphene; *p*-rGO NCs: porous reduced graphene oxide nanosheets; PSS: poly (styrene sulfonate); rGO:Reduced graphene oxide; $SrTiO_3$:perovskite-type strontium titanate; sulfonated-G: Sulfonated graphene; ZnONSt: zinc oxide nanostar; Zr-BDC: zirconium-based metal organic framework material.

6. Electrochemical enzymatic nanobiosensors of pesticides

AChE biosensors have emerged as highly simple, rapid, and ultra-sensitive/selective technique for pesticide residue monitoring in water and soils sources. Pesticides inhibit the acetylcholinesterase, which is a biorecognition element by phosphorylation of its active site. The detection mechanism usually depends on the AChE catalyzed reaction of acetylthiocholine to produce the electro-active thiocholine. The current is enzymatically generated by the electrochemical oxidation of thiocholine. Therefore, it can be used for quantitative measurement of enzyme activity, which is an indicator of the biological effect of pesticides.

AChE should be effectively immobilized on the surface of the modified electrode. The adsorption, covalence, entrapment, cross-linking, and affinity strategies are given as an example for immobilization (Pérez-Fernández et al., 2020). As shown in Table 3, many publications on enzymatic inhibition-based nanobiosensor to analyze pesticides have been reported in the last years.

Wang K. et al. developed an enzymatic electrochemical biosensor based on TiO_2-decorated graphene nanohybrids prepared by *in situ* technique for electrochemical detection of carbaryl (K. Wang et al., 2011a). The proposed amperometric biosensor showed a good performance for pesticide detection, including good reproducibility and acceptable stability. It was effectively utilized to detect carbaryl in the range between 0.001 and 2.0 μgmL^{-1} with a detection limit of 0.74 pgmL^{-1}. For characterization, the AChE-TiO_2-G/GCE was displayed by means of the SEM, TEM, and EIS.

Bao J. et al. have designed a sensitivity electrochemical AChE biosensor to determine malathion, which is the pesticide model of this study (Bao et al., 2019). The authors used three-dimensional graphene-copper oxide nanoflowers (3DG-CuO) nanocomposites to increase the effective specific surface area and improve the biosensor performance. Moreover, under optimized conditions, the calibration curve was obtained linearly in the concentration ranges of 3 pM–46.65 nM with the detection limit of 0.92 pM. This sensor was applied in Yangtze River and Minzhu Lake. The reproducibility of a developed nanobiosensor with a relative standard deviation (RSD) of 4.7% is an acceptable parameter. Stability study shows that excellent storage stability of the biosensor still retains 93.7% after 20 days.

In another work, Zhang P. et al. initiated an electrochemical sensing technique to determine malathion and trichlorfon in the tap water and apple sample (Zhang et al., 2019b). As seen Fig. 2., firstly, the GCE surface was polymerized with 4, 7-di (furan-2-yl) benzo thiadiazole. Then, the Ag-rGO-NH_2 nanocomposite was coated on the GCE before immobilization of AChE. The authors went on to create an AChE

Table 2
The applications of graphene-based nanobiosensor to analyze pesticides.

Analyte	Method	Enzyme electrode	Linear range	LOD	Recovery	Applications	Reference
Parathion	EIS	Anti-parathion antibody/GR/SPE	0.1–1000 ngL^{-1}	52 pgL^{-1}	92–113%	Tomato Sample Carrot Sample	Mehta et al. (2016)
Methyl Parathion	SWV	GR–CS/GCE	4- 400 $ngmL^{-1}$	0.8 $ngmL^{-1}$	–	–	Yang et al. (2012)
Paraquat	DPV	PPY-g-NGE/GCEs	0.05–2 μM	0.041 μM	97.40–98.20%	Ground Water Sample Lake Water Sample	(Li et al., 2015a)
Carbaryl	SWV	GO-IL/GCE	0.10–12.0 μM	0.02 μM	90.0–96.7%	Graphes Sample Tomato Sample	(Liu et al., 2015a)
Phoxim	CV	P3MT/NGE/GCE	0.02–0.2 μM 0.2–2.0 μM	6.4 nM	97.4–101.7%	River Water Sample Tap Water Sample	Wu et al. (2015)
Methyl Parathion	SWV	GN-AuNRs/GCE	10-500 $ngmL^{-1}$ 750-4000 $ngmL^{-1}$	0.82 $ngmL^{-1}$	83.3–107%	Tap Water Sample Kiwi Sample	Zhu et al. (2014)
Imidacloprid	LSV	MIP/rGO/GCE	7.5×10^{-7}-$7x10^{-5}$ M	4×10^{-7}M	91.3–96.6%	Pear Sample	Kong et al. (2013)
Napropamide	ECL	Nafion/sulfonated-G/GCE	10^{-1}-10^{4} $ngmL^{-1}$	1 $ngmL^{-1}$	89.8–115.4%	River Sample	Wang et al. (2014)
P-Nitrophenol	DPV	Graphene/SPE MWCNT/SPE	10 μM-0.62 mM 25 μM-0.62 mM	0.6 μM 1.3 μM	–	Phosphate Buffer Solution (pH 7.0)	Arvinte et al. (2011)
Parathion	CV	Au–Pd/rGO/CPE	0.01–11.2 μM	0.008 μM	96.0–104.2%	Cucumber Sample Cabbage Sample Groundwater Sample Tap Water Sample	Jahromi et al. (2020)
Diazinon	SWV	Au–Pd/rGO–MWCNTs/GCE	0.009–11.3 μM	0.002 μM	96–105%	Water Sample Apple Sample Cucumber Sample	Tadayon and Jahromi (2020)
Metolcarb	DPV	g-C_3N_4/GO/Fc-TED/GCE	0.045–213 μM	8.3 nM	–	Spinach Sample	Xiao et al. (2020)
Methyl Parathion	DPV	ZnONSt@GO/SPCE	0.03–670 μM	1.2 nM	98.0–98.5%	Apple Sample Brocco Flower Sample Collard Greens Sample	Manavalan et al. (2020)
Malathion	DPV	PA_6/PPy/CRGO	500–2×10^4 $ngmL^{-1}$	0.8 $ngmL^{-1}$	99–105%	Tap Water Sample River Water	Migliorini et al. (2019)
Binaphthol	DPV	PtNPs-MoS_2-rGO/GCE	0.4–10 μM 10–40 μM	0.07 μM	98.7–102.9%	Tap Water	Zuo et al. (2020)
Acetamiprid	SWV	3D-CS/rGO/GCE	0.1 pM-0.1 μM	71.2 fM	96.8–103.6%	Tea Samples	Yi et al. (2020)
Malathion	CV	GO/PANI/GG electrode	0.01–150 μgmL^{-1}	0.003 μgmL^{-1}	80.7–116.5%	Grape Apple Juice	Khoshmanesh et al. (2020)
Diazinon			0.10–150 μgmL^{-1}	0.03 μgmL^{-1}		Tomato Samples.	
Phosalone			0.10–300 μgmL^{-1}	0.03 μgmL^{-1}			
Chlorpyrifos			0.10–80 μgmL^{-1}	0.03 μgmL^{-1}			
İmidacloprid	DPV	MIP/Au/rGO/SPCE	–	0.5 μM	98.32–102.2% 99.86–107.5% 100.24–109%	Mango Sample Cowpea Sample Water Sample	Peng et al. (2021)
2,4-Dichlorophenol	DPV	rGO/TiO_2/GCE	5–150 μM	0.02 μM	–	*Artemia Salina*	Ramanathan et al. (2021)
Carbaryl	LSV	RGO grid electrode	0.25–128 mgL^{-1}	0.1 mgL^{-1}	92.0–107.0%	Apple Juice Orange Juice	Saqib et al. (2021)
Methyl Parathion	SWV	GNPs/Zirconia/SPE	1–20 μM 20–50 μM	0.1 μM	92.6–89.4%	Acetate Buffer	Ulloa et al. (2021)
Carbamate	DPV	$Dy_2Sn_2O_7$/GO/SPE	0.05–124.65 μM	14.8 nM	96.5–99.9%	Cabbage Sample Carrot Sample Potato Sample Eggplant Sample	Thirumalraj et al. (2020)
Carbendazim	DPV	rGO/B/CPE	30–900 nM	2.3 nM	77.7–122.0%	Orange Juice Lettuce Leaves Drinking Water Wastewater	Sant et al. (2020)
Pentachlorophenol	DPV	AgNPs-rGO/GCE	0.008–10.0 μM	0.001 μM	94.0–108.0%	Drinking Water	(Wang et al., 2020c)
Carbofuran	DPV	$(PDDA/ERGO)_5$/$(MNP/PSS)_5$/ITO	0.83–11.4 μM	0.407 μM	101-97%	Tap Water Soil	Miyazaki et al. (2020)
Deltamethrin	CV	rGO-PEI-AgNPs/GCE	10 nM-1 mM	10 nM	–	Human Plasma Sample	Adel et al. (2021)
Trifluralin	Amperometric	Au@Ag cores-shell/GQDs ink/glove	10 nM-1 mM	10 nM	–	Leaf Sample Apple Samples	Mahmoudpour et al. (2021)
Furaltadone	Amperometric	FeVO/p-rGO NCs/GCE	0.5–84 μM 94–1319 μM	138 nM	98.2–101.5%	İndustrial Wastewater Lake Water Samples	Rajakumaran et al. (2021)
Methyl Parathion	Amperometric	Ag@GNRs/SPE	2 nM–2525 μM 4 nM–2400 μM 6 nM–1700 μM 4 nM–2080 μM	1 nM 2.0 nM 2.0 nM 3.0 nM	–	Cabbage Sample Green Beans Sample Strawberry Sample Nectarine Sample	Govindasamy et al. (2017)
Profenofos Phorate İsocarbophos Omethoate	DPV	Aptamer/rGO-CuNPs/SPE	0.01–100 nM 1–1000 nM 0.1–1000 nM 1–500 nM	0.003 nM 0.3 nM 0.03 nM 0.3 nM	96.2–118.8%	Rape Sample Spinach Sample	Fu et al. (2019)
Cyhexatin	DPV	MIP-AuNPs/ERGO/SPE	1-500 $ngmL^{-1}$	0.20 $ngmL^{-1}$	79.6–92.1%	Pear Samples	(Zhang et al., 2019a)
Methyl Parathion	SWV	Zr-BDC-rGO/GCE		0.5 $ngmL^{-1}$	95.3–103.4%	Chinese Cabbage Sample	Gao et al. (2021)

(*continued on next page*)

Table 2 (*continued*)

Analyte	Method	Enzyme electrode	Linear range	LOD	Recovery	Applications	Reference
			0.001–3.0 μgmL^{-1}				
Imidacloprid	LSV	rGO/CD/GCE	0.5–40 μM	0.02 μM	92–99%	Brown Ice Sample	Zhao et al. (2020)
Parathion		ZrO_2/rGO/GCE	10 $pgmL^{-1}$-10 μgmL^{-1}	10 $pgmL^{-1}$	87–118%	Chinese Cabbage Sample	Tao et al. (2021)
Methyl Parathion	DPV	GO@Ce-doped TiO_2NPs/GCE	0.002–48.327 μM	0.0016 μM	98.2–99.5%	Apple Sample Tomato Sample	Nehru et al. (2021)
Isoproturon	CV	CNT/CuO/CPE	1 -200 μgL^{-1}	0.1 μgL^{-1}	96.4–101.7%	Tap Water Sample	Amra et al. (2020)
Glyphosate	DPV	MIPNs/SPE	2.5–350 $ngmL^{-1}$	1.94 $ngmL^{-1}$	97.5–101.7%, 94.54–102.7%	Orange Juice Sample Rice Beverage Sample	Ding et al. (2021)
Amitrole	DPV	N-CMK-5/GCE	0.02–0.25 mM	0.007 mM	96.7–105.0%	River Water Sample	Zhou et al. (2021)
Methyl Parathion	DPV	N-HG_{50}/GCE	1-150 $ngmL^{-1}$	3.5 $pgmL^{-1}$	99–102%	Apple Sample Grape Sample Cucumber Sample River Water Sample	(Chen et al., 2021b)
2,4,6-Trichlorophenol	CV	GO@$SrTiO_3$-NC/GCE	0.01–1.47 μM 1.47–434.4 μM	3.21 nM	96.4–98.4% 95.4–97.6%	River Water Sample Soil Sample	Akilarasan et al. (2021)
Carbofuran	DPV	Gd_2S_3/RGO/GCE	0.001–1381 μM	0.0128 μM	99.4–99.8%	Potato Stock Solution River Water Sample	Mariyappan et al. (2021)
Chlorpyrifos Dichlorvos Methamidophos Dimethoate Phoxim Parathion Omethoate Pirimiphos Methyl Diazinon Fenthion Trichlorfon Methomyl	DPV	GR/CS/parathion/GCE	1–1500 $ngmL^{-1}$	0.035$ngmL^{-1}$ 0.054$ngmL^{-1}$ 0.065$ngmL^{-1}$ 0.012$ngmL^{-1}$ 0.067$ngmL^{-1}$ 0.079$ngmL^{-1}$ 0.082$ngmL^{-1}$ 0.056$ngmL^{-1}$ 0.230$ngmL^{-1}$ 0.055$ngmL^{-1}$ 0.047$ngmL^{-1}$ 0.330$ngmL^{-1}$	87.24–110.2%	Apple Sample	Xie et al. (2021)
Glyphosate	DPASV	MIP/AuNPs/PGE	3.98–176.2 $ngmL^{-1}$	0.35 $ngmL^{-1}$	97.5–102.3%	Aqueous Sample Human Serum Sample	Prasad et al. (2014)
Glufosinate			0.54–3.96 $ngmL^{-1}$	0.19 $ngmL^{-1}$		Soil Sample	
Carbofuran	DPV	AuNPs/GO/SPE	1–250 μM	0.22 μM	92.8–107.2%	Cucumber Samples Rice Samples	Jirasirichote et al. (2017)
Isoproturon Carbendazim	SWV	GR/Carbon working electrode	0.02–10.0 mgL^{-1} 0.50–10.0 mgL^{-1}	0.02 mgL^{-1} 0.5 mgL^{-1}	81.4–107%	Chao Phraya River Water Sample Rice Sample Soil Sample Tomato Sample Lettuce Sample	Noyrod et al. (2014)
Carbaryl Paraquat	DPV	BDDGR	1–6 μM 0.2–1.2 μM	0.07–0.16 μM 0.02–0.04 μM	–	Apple Juice Sample	Pop et al. (2017)
Imidacloprid	CV	GO/GCE	0.8–10 μM	0.36 μM	94.0–102.5%	Tap Water Sample Lake Water Sample	Lei et al. (2014)

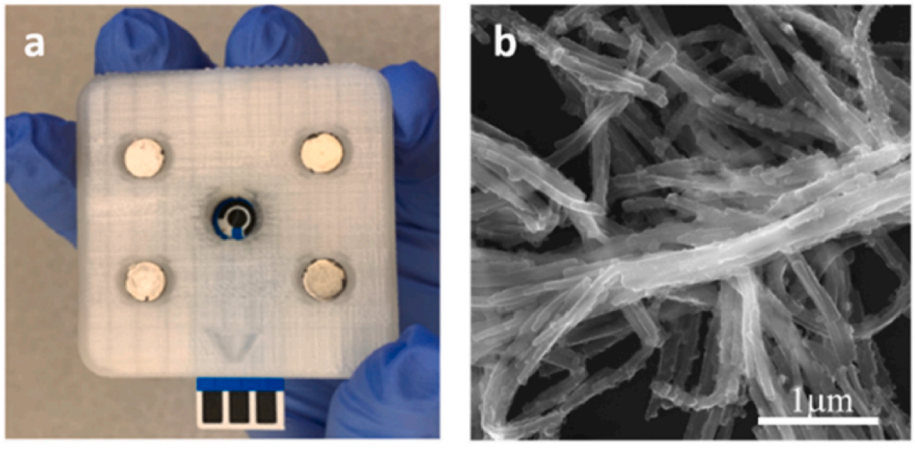


Fig. 1. A)The picture of 3D-printed SPE holder, B) SEM image of MIPNs. Reproduced with permission from Elsevier (Ding et al., 2021).

electrochemical biosensor to obtain acceptable reproducibility (RSD of 2.30% (malathion) and 3.44% (trichlorfon)) and long-term stability (82.7% after 30-days). The malathion and trichlorfon had a detection limit of 0.032 μgmL^{-1} and 0.001 μgmL^{-1} and analytical sensitivity in the range of 0.099–9.9 μgL^{-1} and 0.0206–2.06 μgL^{-1}, respectively.

In Chen D. et al. paper, an electrochemical sensing strategy

Table 3
The applications of AChE inhibition-based nanobiosensor to analyze pesticides.

Analyte	Method	Enzyme electrode	Linear range	LOD	Recovery	Applications	Reference
Carbaryl	Amperometric	AChE/TiO_2-GR/GCE	0.001–0.015μgmL^{-1} 0.015–2 μgmL^{-1}	0.3 ngmL^{-1}	91.8%	0.1 M Phosphate Buffer Solution (Ph 7.0)	(K. Wang et al., 2011a)
Dimethoate	DPV	AChE/IL-GR/Co_3O_4/CS/GCE	5 × 10^{-12} M-1x10^{-7} M	1 × 10^{-13} M	92.5–107.5%	Lettuce Leaf Sample	Zheng et al. (2016)
Paraoxon	Amperometric	AChE/Au–PPy–rGO/GCE	1 nM-5 μM	0.5 nM	–	Tap Water	Yang et al. (2014)
Trichlorfon	DPV	AChE/3D-EUS integrated electrode	0.20–18 ngmL^{-1}	0.069ngmL^{-1}	97.1–104%	–	Zhang et al. (2021)
Monocrotophos	CV	AChE/PAH/MWCNT/CPE	1–25 pgmL^{-1}	0.88 pgmL^{-1}	98–101%	Tap Water Mineralized Water Tomato Grape	Çevik et al. (2013)
Methyl Parathion	Amperometric	AChE/rGO/PDA/AuNPs/ AgNPs/CS/GCE	0.076–3040 nM	9.1 pM	–	PBS Buffer (pH 7.4)	Chen et al. (2019)
Paraoxon Dichlorvos	Amperometric	AChE/GR/CdSe@ZnS electrode	10^{-12}–10^{-6} M	10^{-14} M 10^{-12} M	93.6–103.3%	Apple Sample	(Li et al., 2015b)
Monocrotophos	SWV	AChE/CS/ZnONPs/rGO/Au Electrode	0.01–100 nM	0.01 nM	98.0–99.5%	Visceral Sample	Singh et al. (2020)
Paraoxon	Amperometric	AChE/AuNPs/rGO/GCE	0.1 pM-5 nM	0.1 pM	–	10 mM Phosphate Buffer (pH 7.4)	(Wang et al., 2011c)
Paraoxon	Amperometric	AChE/Ce/UiO-66/MWCNTs/ GCE	0.01–150 nM	0.004 nM	95–102%	Cabbage Sample Spinach Sample	Mahmoudi et al. (2019)
Methyl Parathion Chlorpyrifos	CV	AChE/PANI-MWCNT/ITO	10-120 ngL^{-1}	8.8 ngL^{-1}	93.0–99.75%	Cucumber Sample	Nagabooshanam et al. (2020)
Malathion, Methyl Parathion Chlorpyrifos Dufulin	ECL	AChE/ChOx/Pt–Au/MWCNT/ GCE	50–500 nM	0.16 nM 0.09 nM 0.08 nM 29.7 nM	78–108%	Cabbage Sample	Miao et al. (2016)
Dichlorvos	Amperometric	AChE/ERGO/Nafion/GCE	5.0–100 ngmL^{-1} 1.0–20 ngmL^{-1}	2.0 ngmL^{-1}	92–108%	River Water Sample	Wu et al. (2013)
Carbaryl	Amperometric	AChE/e-GON/GCE	0.3–6.1 ngmL^{-1}	0.15 ngmL^{-1}	98.3–102.2%	Cabbage Sample Spinach Sample	Li et al. (2017a)
Carbaryl	Amperometric	AChE/MWCNTs/GONR/GCE	5–5000 nM	1.7 nM	95.5%–96.8%	Cabbage Samples	(Liu et al., 2015b)
Phorate	DPV	AChE/IL/GR/PVA/GCE	1 × 10^{-14}-1x10^{-9} M 1 × 10^{-9}-1x10^{-6} M	8 × 10^{-15} M	92.0–107.5%	Apple Juice	Zheng et al. (2015b)
Malathion Methidathion Chlorpyrifos Ethyl	Amperometric	AChE/Nafion/Ag@rGO-NH_2/ GCE	6.3–77 ngmL^{-1} 12-105 ngmL^{-1} 21-122 ngmL^{-1}	4.5 ngmL^{-1} 9.5 ngmL^{-1} 14 ngmL^{-1}	90.57–109.7%	Tap Water Samples	Guler et al. (2017)
Carbaryl	DPV	AChE/rGO/GCE	10-50 ngmL^{-1}	1.9 ngmL^{-1}	–	Tomato Samples	da Silva et al. (2018)
Carbaryl	CV	AChE/CdS/GR/CS/GCE	2 ngmL^{-1}-2 μgmL^{-1}	0.7 ngmL^{-1}	–	0.1 M Phosphate Buffer (pH 7.0)	(K. Wang et al., 2011b)
Phoxim	DPV	AChE/CS/AgNC/rGO/GCE	0.2–250 nM	81 pM	89.7–96.6%	Water Samples	Zhang et al. (2015)
Monocrotophos	DPV	Cl/MWCNTs/HRP/AChE/ GCE	1 × 10^{-11}- 1 × 10^{-7} M	4.5 × 10^{-12} M	83.0–104.0%	Cabbage Sample	Jiaojiao et al. (2020)
Malathion	DPV	AChE/Fe_3O_4@MHCS/GCE	0.01–50 ppb 50–600 ppb	0.0182 ppb	97.80–104.1%	Pear Sample	Luo et al. (2018)
Methyl Parathion	SWV	AChE/ERGO-Nf/GCE	2 × 10^{-9}-7x10^{-7} M	1 × 10^{-9} M	90%	Potato Samples.	Jeyapragasam et al. (2017)
Methyl Parathion	SWV	BSA/AChE-Glu-s-SWCNTs/ GCE	1 × 10^{-10}-5x10^{-6} M	3.8 × 10^{-11} M	98.31–102.2%	Strawberry Sample Apple Sample	Kumar and Sundramoorthy (2019)
Paraoxon	DPV	AChE/HGO/GCE	10-45 ngmL^{-1}	1.58 ngmL^{-1}	96.9–100.4%	Lettuce Sample Cabbage Sample	Li et al. (2018)
Chlorpyrifos	CV	AChE/MWCNTs/IL/SPE	0.05–1x10^{5} μM	0.05 μM	87–101%	Cabbage Sample Rapr Sample Lettuce Sample	Chen et al. (2017a)
Carbaryl	DPV	AChE/PDDA/MWCNTs/GR/ GCE	0.8–50 ngmL^{-1} 50-3000 ngmL^{-1}	0.13 ngmL^{-1}	92.3–107%	Cabbage Sample Garland Chrysanthemum Sample Leek Sample Pakchoi Sample	Sun et al. (2013)
Monocrotophos	SWV	AChE –PBNCs/rGO/SPE	1-600 ngmL^{-1}	0.1 ngmL^{-1}	97–104%	Cucumber Sample	Zhang et al. (2012)
Chlorpyrifos	DPV	CLDH-AChE/GR-AuNPs/GCE	0.05–150 μg L^{-1}	0.05 μgL^{-1}	96.5–107.1%	Leek Sample Pakchoi Sample	Zhai et al. (2014)
Phosmet	CV	AChE/WO_3/GCN/PGE	5–125 nM	3.6 nM	99.0%	Wheat Flour Sample	Bilal et al. (2021)
Chlorpyrifos	DPV	AChE/AuNCs/GO/CS/SPE	0.01–500 μgL^{-1}	3 ngL^{-1}	96.1–101.7%	Oilseeed Sample Lettuce Sample Rape Sample Spinach Sample	Yao et al. (2019)
Dimethoate	CV			2 nM	98.5–102.2%	Garlic Sample	Du et al. (2010b)

(*continued on next page*)

Table 3 (*continued*)

Analyte	Method	Enzyme electrode	Linear range	LOD	Recovery	Applications	Reference
		AChE/MWCNTs/β-CD/CS/GCE	0.01–2.44 μM 2.44–10.00 μM				
Dimethoate	DPV	AChE/CNT/ZrO_2/PB/Nafion/GMP/SPE	1×10^{-3}–10 $ngmL^{-1}$	5.6×10^{-4} $ngmL^{-1}$	88–105%	Cabbage Sample	Gan et al. (2010)
Chlorpyrifos	CV	AChE/MWCNTs/DCHP/SPE	0.05–1.0 × 10^5 μgL^{-1}	0.05 μg/L	–	Cabbage Sample Rape Sample Lettuce Sample	Chen et al. (2017b)
Malathion Trichlorfon	CV	poly (FBThF)/Ag-rGO-NH_2/AChE/GCE	0.099–9.9 μgL^{-1} 0.0206–2.06 μgL^{-1}	0.032 μgL^{-1} 0.001 μgL^{-1}	95.2–108.0%	Tap Water Sample Apple Sample	(Zhang et al., 2019b)
Dichlorvos	DPV	AChE/Ti_3C_2Tx-CS/GR/GCE	22.6 nM-11.31 μM	14.45 nM	98.2–109%	Urban Tap Water Samples	(Wang et al., 2020a)
Trichlorfon	Amperometric	AChE/CS/Au electrode	300 nM-3 μM	10 nM	92.50–98.50%	Rice Samples	(Wang et al., 2021b)
Malathion	Amperometric	AChE-CS/3DG-CuO NFs/GCE	3 pM-46.665 nM	0.93 pM	94–106%	River Sample	Bao et al. (2019)
Chlorpyrifos	DPV	AChE/Fe_3O_4/GR/SPE	0.05 μgL^{-1}-100 μgL^{-1}	0.02 μgL^{-1}	91.1–108.3%	Cabbage Sample Spinach Sample	Wang et al. (2016)
Chlorpyrifos	DPV	Nafion/AChE/MWCNTs-SnO_2- CS/Au	0.05–1.0 μgL^{-1}	0.05 μgL^{-1}	98.7–105.6%	Cabbage Sample Lettuce Sample Leek Sample Pak Choi Sample	Chen et al. (2015)
Carbaryl	Amperometric	MWCNT/PANI/AChE/GCE	9.9–49.6 μM	1.4 μM	97.3–103.4%	Apple Sample	Cesarino et al. (2012)
Methomyl			4.9–29.2 μM	0.95 μM	94.6–101.2% 95.4–101.9%	Cabbage Sample Broccoli Sample	
Chlorpyrifos	Amperometric	AChE/CPBA/AuNPs/rGO/CS/GCE	0.5–10 ppb 10–100 ppb	0.1 ppb	–	Phosphate Buffer Solution (Ph 7.0)	Liu et al. (2011)
Malathion			0.5–10 ppb 20–100 ppb	0.5 ppb			
Carbofuran			0.1–10 ppb 10–100 ppb	0.05 ppb			
Isoprocarb			2–10 ppb 20–150 ppb	0.5 ppb			
Malathion, Chlorpyrifos, Monocrotophos Carbofuran	DPV	AChE/CS–PB–MWNTs–HGN/Au electrode	0.05–75 nM 0.05–75 nM 0.1–50 nM 5–80 nM	0.05 nM 0.05 nM 0.1 M 2.5 nM	94.2–105.9%	Cabbage Sample Lettuce Sample Leek Sample Pakcho Sample	Zhai et al. (2013)
Monocrotophos	DPV	AChE/IL/MWCNTs/GCE	1×10^{-10}-5x10^{-7} M	3.3×10^{-11} M	90–104%	Fresh Vegetable Sample	Bin et al. (2018)
Chlorpyrifos Carbary	DPV	Nafion/AChE–CS/Ag NPs–CGR–Nafion/GCE	1×10^{-13}-1x10^{-8} M 1×10^{-12}-1x10^{-8} M	5.3×10^{-14} M 5.4×10^{-13} M	93.1–105.6%	Tapwater Sample Lakewater Sample	Liu et al. (2014)
Carbofuran Paraoxon	Amperometric	AChE/e-GON/MWCNTs/GCE	0.03–0.81 $ngmL^{-1}$ 0.05–1 $ngmL^{-1}$ 1–104 $ngmL^{-1}$	0.015$ngmL^{-1}$ 0.025$ngmL^{-1}$	94.0–102.4%	Spinach Sample Cabbage Sample Water Sample	Li et al. (2017b)
Carbaryl Monocrotophos	DPV	AChE/GA/IL/GR–Gel/GCE	1×10^{-14}-1x10^{-8} M 1×10^{-13}-5x10^{-8} M	5.3×10^{-15} M 4.6×10^{-14} M	92.5–105.0% 91.2–110.0%	Tomato Juice Sample	Zheng et al. (2015a)
Malathion Chlorpyrifon Monocrotophos Endosulfan	CV	AChE/Fe_3O_4NPs/MWCNTs/ITO-coated glass plate	0.1–70 nM 0.1–50 nM 0.1–70 nM 0.1–100 nM	0.1 nM	98.7–104.9%	Cabbage Sample Onion Sample Spinach Sample	Chauhan and Pundir (2012)
Parathion Chlorpyrifos Dichlorvos Methamidophos Dimethoate Phoxim Omethoate Pirimiphosmethyl Diazinon Fenthion Trichlorfon Methomyl	DPV	AChE/AuNPs/mercaptomethamidophos/mercaptohexanol/GCE	0.1–1500 $ngmL^{-1}$	0.03 $ngmL^{-1}$ 0.06 $ngmL^{-1}$ 0.02 $ngmL^{-1}$ 0.03 $ngmL^{-1}$ 0.02 $ngmL^{-1}$ 0.04 $ngmL^{-1}$ 0.03 $ngmL^{-1}$ 0.08 $ngmL^{-1}$ 0.06 $ngmL^{-1}$ 0.04 $ngmL^{-1}$ 0.02 $ngmL^{-1}$ 0.08 $ngmL^{-1}$	81.45–116.8%	Cabbage Sample	Zhao et al. (2021)
Chlorpyrifos Malathion Methyl Parathion	DPV	AChE/PEDOT/rGO/IL/FTO/GCE	–	0.17 $ngmL^{-1}$ 0.18 $ngmL^{-1}$ 0.18 $ngmL^{-1}$ 0.44 $ngmL^{-1}$ 0.20 $ngmL^{-1}$ 11.7 $ngmL^{-1}$	–	Apple Juice Sample Aerated Drinks Apple Juice Sample Aerated Drinks Apple Juice Sample Aerated Drinks	Rana et al. (2019)
Fenitrothion	Amperometric	Tyrosinase/poly (2-hydroxybenzamide)/GR Electrode	0.018–3.60 μM	4.70 nM	97.6%	Water Sample	Alves et al. (2018)
Chlorpyrifos	Amperometric	AChE/IL/MWCNT/CPE	10^{-8}–10^{-6} M	4 nM	–	Phosphate Buffer Solution (pH 8.0)	Zamfir et al. (2011)
Dichlorvos	CV	(MWCNTs/ALB)$_6$/GCE	0.25–1.75 l μM 2.00–10.00 μM	0.68 μgL^{-1}	–	Phosphate Buffered Saline (pH 7.0)	Yan et al. (2013)
Dichlorvos	DPV	AChE/CS@TiO_2-CS/rGO/GCE	0.036–22.6 μM	29 nM	100%	Cabbage Juice Sample	Cui et al. (2018)

3D-EUS: 3D porous Eucommia ulmoides; 3DG-CuO NFs: three dimensional graphene-copper oxide nanoflowers nanocomposites; ALB: AChE liposomes bioreactor; CGR: Carboxylic graphene; CLDH: Cu–Mg–Al calcined layered double hydroxide; CPBA: 3-carboxyphenylboronic acid; DCHP: dicyclohexyl phthalate; e-GON: 3D graphene oxide network; FBThF: 4, 7-di (furan-2-yl) benzo thiadiazole; GA: Gluteraldehide; GCN: g-C3N4; GMP: Fe_3O_4/Au magnetic nanoparticulate; HGN: hollow gold nanospheres; HRP: horseradish peroxidase; PAH: Poly(allylamine hydrochloride); PB: prussian blue; PBNCs: Prussian blue nanocube; PDA: polydopamine; PDDA: Poly (diallyldimethylammonium chloride); PEDOT: poly(3,4- ethylenedioxythiophene); PPy: polypyrrole; PVA: polyvinyl alcohol; WO_3: tungsten trioxide; ZnONFs: Zinc oxide nanoflowers.

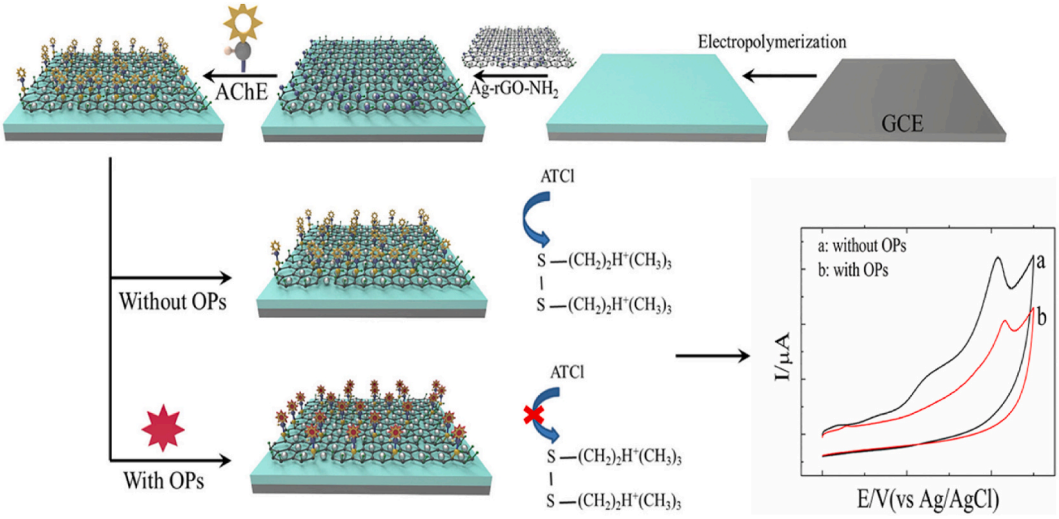


Fig. 2. The illustration of fabratication of enzymatic biosensor. Reproduced with permission from Elsevier (Zhang et al., 2019b).

comprising a multi-walled carbon nanotubes/dicyclohexyl phthalate modified screen-printed electrode has been reported to determine chlorpyrifos (Chen et al., 2017b). The proposed electrochemical sensor showed a linear response for chlorpyrifos in the concentration range of 0.05–1.0 × 10^5 μgL^{-1} with a detection limit value of 0.05 μgL^{-1}. Furthermore, under the optimal experimental conditions, chlorpyrifos in cabbage, rape, and lettuce was quantitatively analyzed with good reproducibility and acceptable stability (82% after 30-days storage).

7. Conclusion

This work mainly focuses on three aspects: 2D-carbon nanomaterials, pesticides, and application of CNT-based electrochemical biosensors, GR-based electrochemical biosensors, and enzymatic nanobiosensors. A wide variety of analysis methods are developed to enhance the sensitive and selective determination of pesticides. Mainly, the carbon nanomaterials such as CNTs or GR derivatives, which acted as immobilization matrices of enzymes and conductive electrode surfaces, have been observed in many studies. The synergistic effects occur through the relationship between carbon-based nanomaterials and noble metal nanoparticles or polymers. As shown in the tables, the synergistic effect enhances the better detection of pesticides in electrochemical nanobiosensors. AChE is one of the most commonly used enzymes for the determination of pesticides. Recently, carbon-based nanomaterials with electrical and physical properties have increased the efficient fabrication of enzyme biosensors. However, the severe instability problem could not be overcome in most reported AChE electrochemical biosensors.

8. Future outlook

Future efforts will investigate the more stable recognition elements to satisfy the long-time monitoring and efficient on-site analysis. Extensive research should be conducted on new surface nanostructuring strategies between enzymes and nanomaterials. The electrochemical performance of amperometric enzyme electrodes enhances with 2D carbon nanomaterials as substrates. Biosensors based on enzyme immobilization with improved performance can be conducted to invent more effective constructing techniques. 2D carbon nanomaterials display greater electron transfer capabilities in electrochemical reactions.

Moreover, the intelligent-wearable biosensor can be developed for the in-situ determination of pesticides in water and soil samples. Therefore, the intelligent-wearable biosensor can give pesticide residue information in a very short time.

The major challenge for the environmental application of biosensors is to translation the technologies from the support electrolyte to real-world environmental samples such as water and solid sources. Challenges to be overcome include sample preparation, matrix effects, and system integration. The system integration challenges can be overcome by the integration of sensing technology with 2-dimensional nanomaterials, possessing a high surface-to-volume ratio, good conductivities, shock-bearing abilities, and color tunability. Some of the problems of conventional sample preparation can solve with simplification and automation. Matrix effects can dramatically influence analysis performance for both identification and quantification of a pesticide analyte. The developments in biosensors using disposable screen-printed carbon electrodes have provided low-cost and reliable assays for rapid electrochemical measurements of pesticides.

Credit author statement

Goksu Ozcelikay: Investigation, Conceptualization, Writing – original draft, **Leyla Karadurmus:** Investigation, Conceptualization, Writing – original draft, **Selva Bilge:** Investigation, Conceptualization, Writing – original draft. **Ali Sınağ;:** Conceptualization, Writing – review & editing. **Sibel A. Ozkan:** Supervision, Conceptualization, Writing – review & editing.

Declaration of competing interest

The authors declare that they have no known competing financial interests or personal relationships that could have appeared to influence the work reported in this paper.

References

Adel, B., Jafari, M., Hasanzadeh, M., 2021. Utilization of rGO-PEI-supported AgNPs for sensitive recognition of deltamethrin in human plasma samples: a new platform for the biomedical analysis of pesticides in human biofluids. J. Mol. Recogn. 34 https://doi.org/10.1002/JMR.2900.

Agharkar, M., Kochrekar, S., Hidouri, S., Azeez, M.A., 2014. Trends in green reduction of graphene oxides, issues and challenges: a review. Mater. Res. Bull. 59, 323–328. https://doi.org/10.1016/j.materresbull.2014.07.051.

Akilarasan, M., Tamilalagan, E., Chen, S., Maheshwaran, S., 2021. An eco-friendly low-temperature synthetic approach towards micro-pebble-structured GO@SrTiO3 nanocomposites for the detection of 2,4,6-trichlorophenol in environmental samples. Microchim. Acta 188. https://doi.org/10.1007/s00604-021-04729-w.

Allen, M.J., Tung, V.C., Kaner, R.B., 2010. Honeycomb carbon: a review of graphene. Chem. Rev. 110, 132–145. https://doi.org/10.1021/cr900070d.

Alves, M. de F., , Corrêa, R.A.M. de S., da Cruz, F.S., Franco, D.L., Ferreira, L.F., 2018. Electrochemical enzymatic fenitrothion sensor based on a tyrosinase/poly(2-hydroxybenzamide)-modified graphite electrode. Anal. Biochem. 553, 15–23. https://doi.org/10.1016/j.ab.2018.05.014.

Amra, S., Bataille, T., Bourouina Bacha, S., Bourouina, M., Hauchard, D., 2020. Nanostructured modified carbon paste electrode as voltrammetric sensor for isoproturon trace analysis in water. Electroanalysis 32, 1346–1353. https://doi.org/10.1002/elan.201900083.

Arvinte, A., Mahosenaho, M., Pinteala, M., Sesay, A.M., Virtanen, V., 2011. Electrochemical oxidation of p-nitrophenol using graphene-modified electrodes, and a comparison to the performance of MWNT-based electrodes. Microchim. Acta 174, 337–343. https://doi.org/10.1007/s00604-011-0628-x.

Ba Hashwan, S.S., Khir, M.H.B.M., Al-Douri, Y., Ahmed, A.Y., 2020. Recent progress in the development of biosensors for chemicals and pesticides detection. IEEE Access 8, 82514–82527. https://doi.org/10.1109/ACCESS.2020.2991380.

Bachmatiuk, A., Zhao, J., Gorantla, S.M., Martinez, I.G.G., Wiedermann, J., Lee, C., Eckert, J., Rummeli, M.H., 2015. Low voltage transmission electron microscopy of Graphene. Small 11, 515–542. https://doi.org/10.1002/smll.201401804.

Bagheri, H., Afkhami, A., Khoshsafar, H., Hajian, A., Shahriyari, A., 2017. Protein capped Cu nanoclusters-SWCNT nanocomposite as a novel candidate of high performance platform for organophosphates enzymeless biosensor. Biosens. Bioelectron. 89, 829–836. https://doi.org/10.1016/j.bios.2016.10.003.

Bao, J., Hou, C., Dong, Q., Ma, X., Chen, J., Huo, D., Yang, M., Galil, K.H.A. El, Chen, W., Lei, Y., 2016. ELP-OPH/BSA/TiO2 nanofibers/c-MWCNTs based biosensor for sensitive and selective determination of p-nitrophenyl substituted organophosphate pesticides in aqueous system. Biosens. Bioelectron. 85, 935–942. https://doi.org/10.1016/j.bios.2016.05.094.

Bao, J., Huang, T., Wang, Z., Yang, H., Geng, X., Xu, G., Samalo, M., Sakinati, M., Huo, D., Hou, C., 2019. 3D graphene/copper oxide nano-flowers based acetylcholinesterase biosensor for sensitive detection of organophosphate pesticides. Sensor. Actuator. B Chem. 279, 95–101. https://doi.org/10.1016/j.snb.2018.09.118.

Bilal, S., Mudassir Hassan, M., Fayyaz ur Rehman, M., Nasir, M., Jamil Sami, A., Hayat, A., 2021. An insect acetylcholinesterase biosensor utilizing WO3/g-C3N4 nanocomposite modified pencil graphite electrode for phosmet detection in stored grains. Food Chem. 346, 128894. https://doi.org/10.1016/j.foodchem.2020.128894.

Bin, Z., Yanhong, C., Jiaojiao, X., Jing, Y., 2018. Acetylcholinesterase biosensor based on functionalized surface of carbon nanotubes for monocrotophos detection. Anal. Biochem. 560, 12–18. https://doi.org/10.1016/j.ab.2018.08.024.

Caetano, K. dos S., da Rosa, D.S., Pizzolato, T.M., dos Santos, P.A.M., Hinrichs, R., Benvenutti, E.V., Dias, S.L.P., Arenas, L.T., Costa, T.M.H., 2020. MWCNT/zirconia porous composite applied as electrochemical sensor for determination of methyl parathion. Microporous Mesoporous Mater. 309, 110583. https://doi.org/10.1016/j.micromeso.2020.110583.

Castro Neto, A.H., Guinea, F., Peres, N.M.R., Novoselov, K.S., Geim, A.K., 2009. The electronic properties of graphene. Rev. Mod. Phys. 81, 109–162. https://doi.org/10.1103/RevModPhys.81.109.

Cesarino, I., Moraes, F.C., Lanza, M.R.V., MacHado, S.A.S., 2012. Electrochemical detection of carbamate pesticides in fruit and vegetables with a biosensor based on acetylcholinesterase immobilised on a composite of polyaniline-carbon nanotubes. Food Chem. 135, 873–879. https://doi.org/10.1016/j.foodchem.2012.04.147.

Çevik, S., Timur, S., Anik, Ü., 2013. Poly(allylamine hydrochloride) functionalized multiwalled carbon nanotube modified carbon paste electrode as acetylcholinesterase biosensor transducer. Electroanalysis 25, 2377–2383. https://doi.org/10.1002/elan.201300260.

Chauhan, N., Pundir, C.S., 2012. An amperometric acetylcholinesterase sensor based on Fe 3O 4 nanoparticle/multi-walled carbon nanotube-modified ITO-coated glass plate for the detection of pesticides. Electrochim. Acta 67, 79–86. https://doi.org/10.1016/j.electacta.2012.02.012.

Chen, D., Fu, J., Liu, Z., Guo, Y., Sun, X., Wang, X., Wang, Z., 2017a. A Simple acetylcholinesterase biosensor based on ionic liquid/multiwalled carbon nanotubes-modified screen-printed electrode for rapid detecting chlorpyrifos. Int. J. Electrochem. Sci. 12, 9465–9477. https://doi.org/10.20964/2017.10.12.

Chen, D., Liu, Z., Fu, J., Guo, Y., Sun, X., Yang, Q., Wang, X., 2017b. Electrochemical acetylcholinesterase biosensor based on multi-walled carbon nanotubes/dicyclohexyl phthalate modified screen-printed electrode for detection of chlorpyrifos. J. Electroanal. Chem. 801, 185–191. https://doi.org/10.1016/j.jelechem.2017.06.032.

Chen, D., Sun, X., Guo, Y., Qiao, L., Wang, X., 2015. Acetylcholinesterase biosensor based on multi-walled carbon nanotubes-SnO2-chitosan nanocomposite. Bioproc. Biosyst. Eng. 38, 315–321. https://doi.org/10.1007/s00449-014-1270-x.

Chen, X., Wang, J., Liu, Z., Li, Y., Huang, J., Tao, C.A., 2019. One pot fabrication of graphene-bimetallic nanoparticles-based acetylcholinesterase electrochemical biosensor with ultralow detection limit toward methyl parathion. Mater. Res. Express 6, 105093. https://doi.org/10.1088/2053-1591/ab3e84.

Chen, Y., He, K., Sun, F., Wei, D., Li, H., 2021a. Efficient electrochemical sensor based on multi-walled carbon nanotubes/gold nanocomposite for detection of dichlorvos pesticide in agricultural food. Int. J. Electrochem. Sci. 16, 1–12. https://doi.org/10.20964/2021.03.53.

Chen, Z., Zhang, Y., Yang, Y., Shi, X., Zhang, L., Jia, G., 2021b. Hierarchical nitrogen-doped holey graphene as sensitive electrochemical sensor for methyl parathion detection. Sensor. Actuator. B Chem. 336, 129721. https://doi.org/10.1016/j.snb.2021.129721.

Childres, I., Jauregui, L.A., Park, W., Caoa, H., Chena, Y.P., 2013. Raman spectroscopy of graphene and related materials. In: New Developments in Photon and Materials Research, pp. 403–418.

Chuntib, P., Themsirimongkon, S., Saipanya, S., Jakmunee, J., 2017. Sequential injection differential pulse voltammetric method based on screen printed carbon electrode modified with carbon nanotube/Nafion for sensitive determination of paraquat. Talanta 170, 1–8. https://doi.org/10.1016/j.talanta.2017.03.073.

Cui, H.F., Wu, W.W., Li, M.M., Song, X., Lv, Y., Zhang, T.T., 2018. A highly stable acetylcholinesterase biosensor based on chitosan-TiO2-graphene nanocomposites for detection of organophosphate pesticides. Biosens. Bioelectron. 99, 223–229. https://doi.org/10.1016/j.bios.2017.07.068.

da Silva, M.K.L., Vanzela, H.C., Defavari, L.M., Cesarino, I., 2018. Determination of carbamate pesticide in food using a biosensor based on reduced graphene oxide and acetylcholinesterase enzyme. Sensor. Actuator. B Chem. 277, 555–561. https://doi.org/10.1016/J.SNB.2018.09.051.

da Silva, W., Ghica, M.E., Brett, C.M.A., 2019. Choline oxidase inhibition biosensor based on poly(brilliant cresyl blue) – deep eutectic solvent/carbon nanotube modified electrode for dichlorvos organophosphorus pesticide. Sensor. Actuator. B Chem. 298, 126862. https://doi.org/10.1016/j.snb.2019.126862.

de Oliveira, G.A., Gevaerd, A., Blaskievicz, S.F., Zarbin, A.J.G., Orth, E.S., Bergamini, M. F., Marcolino-Junior, L.H., 2020. A simple enzymeless approach for Paraoxon determination using imidazole-functionalized carbon nanotubes. Mater. Sci. Eng. C 116, 111140. https://doi.org/10.1016/j.msec.2020.111140.

Demir, E., Göktug, Ö., İnam, R., Doyduk, D., 2021. Development and characterization of iron (III) phthalocyanine modified carbon nanotube paste electrodes and application for determination of fluometuron herbicide as an electrochemical sensor. J. Electroanal. Chem. 895, 115389. https://doi.org/10.1016/j.jelechem.2021.115389.

Ding, S., Lyu, Z., Li, S., Ruan, X., Fei, M., Zhou, Y., Niu, X., Zhu, W., Du, D., Lin, Y., 2021. Molecularly imprinted polypyrrole nanotubes based electrochemical sensor for glyphosate detection. Biosens. Bioelectron. 191, 113434. https://doi.org/10.1016/j.bios.2021.113434.

Du, D., Chen, W., Zhang, W., Liu, D., Li, H., Lin, Y., 2010a. Covalent coupling of organophosphorus hydrolase loaded quantum dots to carbon nanotube/Au nanocomposite for enhanced detection of methyl parathion. Biosens. Bioelectron. 25, 1370–1375. https://doi.org/10.1016/j.bios.2009.10.032.

Du, D., Wang, M., Cai, J., Zhang, A., 2010b. Sensitive acetylcholinesterase biosensor based on assembly of β-cyclodextrins onto multiwall carbon nanotubes for detection of organophosphates pesticide. Sensor. Actuator. B Chem. 146, 337–341. https://doi.org/10.1016/j.snb.2010.02.053.

Fei, A., Liu, Q., Huan, J., Qian, J., Dong, X., Qiu, B., Mao, H., Wang, K., 2015. Label-free impedimetric aptasensor for detection of femtomole level acetamiprid using gold nanoparticles decorated multiwalled carbon nanotube-reduced graphene oxide nanoribbon composites. Biosens. Bioelectron. 70, 122–129. https://doi.org/10.1016/j.bios.2015.03.028.

Fozing Mekeuo, G.A., Despas, C., Péguy Nanseu-Njiki, C., Walcarius, A., Ngameni, E., 2021. Preparation of functionalized ayous sawdust-carbon nanotubes composite for the electrochemical determination of carbendazim pesticide. Electroanalysis 1–11. https://doi.org/10.1002/elan.202100262.

Fu, J., An, X., Yao, Y., Guo, Y., Sun, X., 2019. Electrochemical aptasensor based on one step co-electrodeposition of aptamer and GO-CuNPs nanocomposite for organophosphorus pesticide detection. Sensor. Actuator. B Chem. 287, 503–509. https://doi.org/10.1016/j.snb.2019.02.057.

Gan, N., Yang, X., Xie, D., Wu, Y., Wen, W., 2010. A disposable organophosphorus pesticides enzyme biosensor based on magnetic composite nano-particles modified screen printed carbon electrode. Sensors 10, 625–638. https://doi.org/10.3390/s100100625.

Gao, N., Tan, R., Cai, Z., Zhao, H., Chang, G., 2021. A novel electrochemical sensor via Zr-based metal organic framework – graphene for pesticide detection. J. Mater. Sci. https://doi.org/10.1007/s10853-021-06436-6.

Garcia, L.L.C., Figueiredo-Filho, L.C.S., Oliveira, G.G., Fatibello-Filho, O., Banks, C.E., 2013. Square-wave voltammetric determination of paraquat using a glassy carbon electrode modified with multiwalled carbon nanotubes within a dihexadecylhydrogenphosphate (DHP) film. Sensor. Actuator. B Chem. 181, 306–311. https://doi.org/10.1016/j.snb.2013.01.091.

Geim, A.K., 2012. Graphene prehistory. Phys. Scripta T146, 014003. https://doi.org/10.1088/0031-8949/2012/T146/014003.

Govindasamy, M., Mani, V., Chen, S.M., Chen, T.W., Sundramoorthy, A.K., 2017. Methyl parathion detection in vegetables and fruits using silver@graphene nanoribbons nanocomposite modified screen printed electrode. Sci. Rep. 7, 1–11. https://doi.org/10.1038/srep46471.

Guex, L.G., Sacchi, B., Peuvot, K.F., Andersson, R.L., Pourrahimi, A.M., Ström, V., Farris, S., Olsson, R.T., 2017. Experimental review: chemical reduction of graphene oxide (GO) to reduced graphene oxide (rGO) by aqueous chemistry. Nanoscale 9, 9562–9571. https://doi.org/10.1039/c7nr02943h.

Guler, M., Turkoglu, V., Basi, Z., 2017. Determination of malation, methidathion, and chlorpyrifos ethyl pesticides using acetylcholinesterase biosensor based on Nafion/Ag@rGO-NH2 nanocomposites. Electrochim. Acta 240, 129–135. https://doi.org/10.1016/j.electacta.2017.04.069.

Habekost, A., 2017. Rapid and sensitive spectroelectrochemical and electrochemical detection of glyphosate and AMPA with screen-printed electrodes. Talanta 162, 583–588. https://doi.org/10.1016/j.talanta.2016.10.074.

Han, L., Chen, D., Li, F., 2018. Rational integration of biomineralization, microbial surface display, and carbon nanocomposites: ultrasensitive and selective biosensor for traces of pesticides. Adv. Mater. Interfac. 5, 1–8. https://doi.org/10.1002/admi.201801332.

Hou, W., Shi, Z., Guo, Y., Sun, X., Wang, X., 2017. An interdigital array microelectrode aptasensor based on multi-walled carbon nanotubes for detection of tetracycline. Bioproc. Biosyst. Eng. 40, 1419–1425. https://doi.org/10.1007/s00449-017-1799-6.

Hua, Q.T., Ruecha, N., Hiruta, Y., Citterio, D., 2019. Disposable electrochemical biosensor based on surface-modified screen-printed electrodes for organophosphorus pesticide analysis. Anal. Methods 11, 3439–3445. https://doi.org/10.1039/c9ay00852g.

Huang, X., Yin, Z., Wu, S., Qi, X., He, Q., Zhang, Q., Yan, Q., Boey, F., Zhang, H., 2011. Graphene-based materials: synthesis, characterization, properties, and applications. Small 7, 1876–1902. https://doi.org/10.1002/smll.201002009.

Jahromi, M.N., Tayadon, F., Bagheri, H., 2020. A new electrochemical sensor based on an Au- Pd/reduced graphene oxide nanocomposite for determination of Parathion. Int. J. Environ. Anal. Chem. 100, 1101–1117. https://doi.org/10.1080/03067319.2019.1649398.

Jeyapragasam, T., Saraswathi, R., Chen, S.M., Chen, T.W., 2017. Acetylcholinesterase biosensor for the detection of methyl parathion at an electrochemically reduced graphene oxide-nafion modified glassy carbon electrode. Int. J. Electrochem. Sci. 12, 4768–4781. https://doi.org/10.20964/2017.06.77.

Jiaojiao, X., Bin, Z., Pengyun, W., Qing, L., Xin, S., Rui, J., 2020. Acetylcholinesterase biosensors based on ionic liquid functionalized carbon nanotubes and horseradish peroxidase for monocrotophos determination. Bioproc. Biosyst. Eng. https://doi.org/10.1007/s00449-019-02226-2.

Jirasirichote, A., Punrat, E., Suea-Ngam, A., Chailapakul, O., Chuanuwatanakul, S., 2017. Voltammetric detection of carbofuran determination using screen-printed carbon electrodes modified with gold nanoparticles and graphene oxide. Talanta 175, 331–337. https://doi.org/10.1016/j.talanta.2017.07.050.

Joshi, K.A., Prouza, M., Kum, M., Wang, J., Tang, J., Haddon, R., Chen, W., Mulchandani, A., 2006. V-type nerve agent detection using a carbon nanotube-based amperometric enzyme electrode. Anal. Chem. 78, 331–336. https://doi.org/10.1021/ac051052f.

Joshi, K.A., Tang, J., Haddon, R., Wang, J., Chen, W., Mulchandani, A., 2005. A disposable biosensor for organophosphorus nerve agents based on carbon nanotubes modified thick film strip electrode. Electroanalysis 17, 54–58. https://doi.org/10.1002/elan.200403118.

Jubete, E., Elechowska, K., Loaiza, O.A., Lamas, P.J., Ochoteco, E., Farmer, K.D., Roberts, K.P., Biernat, J.F., 2011. Derivatization of SWCNTs with cobalt phthalocyanine residues and applications in screen printed electrodes for electrochemical detection of thiocholine. Electrochim. Acta 56, 3988–3995. https://doi.org/10.1016/j.electacta.2011.01.123.

Khoshmanesh, M.S., Hamishehkar, H., Razmi, H., 2020. Trace analysis of organophosphorus pesticide residues in fruit juices and vegetables by an electrochemically fabricated solid-phase microextraction fiber coated with a layer-by-layer graphenized graphite/graphene oxide/polyaniline nanocomposite. Anal. Methods 12, 3268–3276. https://doi.org/10.1039/d0ay00626b.

Khosropour, H., Rezaei, B., Rezaei, P., Ensa, A.A., 2020. Ultrasensitive voltammetric and impedimetric aptasensor for diazinon pesticide detection by VS 2 quantum dots-graphene nanoplatelets/carboxylated multiwalled carbon nanotubes as a new group nanocomposite for signal. Enrichment 1111, 92–102. https://doi.org/10.1016/j.aca.2020.03.047.

Kilele, J.C., Chokkareddy, R., Redhi, G.G., 2021. Ultra-sensitive electrochemical sensor for fenitrothion pesticide residues in fruit samples using IL@CoFe2O4NPs@MWCNTs nanocomposite. Microchem. J. 164, 106012. https://doi.org/10.1016/j.microc.2021.106012.

Köksoy, B., Akyüz, D., Şenocak, A., Durmuş, M., Demirbaş, E., 2021. Novel SWCNT-hybrid nanomaterial functionalized with subphthalocyanine substituted asymmetrical zinc (II) phthalocyanine conjugate: design, synthesis, characterization and sensor properties for pesticides. Sensor. Actuator. B Chem. 329 https://doi.org/10.1016/j.snb.2020.129198.

Kong, L., Jiang, X., Zeng, Y., Zhou, T., Shi, G., 2013. Molecularly imprinted sensor based on electropolmerized poly(o-phenylenediamine) membranes at reduced graphene oxide modified electrode for imidacloprid determination. Sensor. Actuator. B Chem. 185, 424–431. https://doi.org/10.1016/j.snb.2013.05.033.

Kumar, T.H.V., Sundramoorthy, A.K., 2019. Electrochemical biosensor for methyl parathion based on single-walled carbon nanotube/glutaraldehyde crosslinked acetylcholinesterase-wrapped bovine serum albumin nanocomposites. Anal. Chim. Acta 1074, 131–141. https://doi.org/10.1016/j.aca.2019.05.011.

Le, V.T., Vasseghian, Y., Dragoi, E.N., Moradi, M., Mousavi Khaneghah, A., 2021. A review on graphene-based electrochemical sensor for mycotoxins detection. Food Chem. Toxicol. 148, 111931. https://doi.org/10.1016/j.fct.2020.111931.

Lei, W., Han, Z., Si, W., Hao, Q., Zhang, Y., Xia, M., Wang, F., 2014. Sensitive and selective detection of imidacloprid by graphene-oxide-modified glassy carbon electrode. Chemelectrochem 1, 1063–1067. https://doi.org/10.1002/celc.201300244.

Li, J., Lei, W., Xu, Y., Zhang, Y., Xia, M., Wang, F., 2015a. Fabrication of polypyrrole-grafted nitrogen-doped graphene and its application for electrochemical detection of paraquat. Electrochim. Acta 174, 464–471. https://doi.org/10.1016/j.electacta.2015.06.028.

Li, M., Mu, B., 2019. Effect of different dimensional carbon materials on the properties and application of phase change materials: a review. Appl. Energy 242, 695–715. https://doi.org/10.1016/j.apenergy.2019.03.085.

Li, X., Zheng, Z., Liu, X., Zhao, S., Liu, S., 2015b. Nanostructured photoelectrochemical biosensor for highly sensitive detection of organophosphorous pesticides. Biosens. Bioelectron. 64, 1–5. https://doi.org/10.1016/j.bios.2014.08.006.

Li, Y., Shi, L., Han, G., Xiao, Y., Zhou, W., 2017a. Electrochemical biosensing of carbaryl based on acetylcholinesterase immobilized onto electrochemically inducing porous graphene oxide network. Sensor. Actuator. B Chem. 238, 945–953. https://doi.org/10.1016/j.snb.2016.07.152.

Li, Y., Zhao, R., Shi, L., Han, G., Xiao, Y., 2017b. Acetylcholinesterase biosensor based on electrochemically inducing 3D graphene oxide network/multi-walled carbon nanotube composites for detection of pesticides. RSC Adv. 7, 53570–53577. https://doi.org/10.1039/c7ra08226f.

Li, Y.P., Zhao, R.X., Han, G.Y., Xiao, Y.M., 2018. Novel acetylcholinesterase biosensor for detection of paraoxon based on holey graphene oxide modified glass carbon electrode. Electroanalysis 30, 2258–2264. https://doi.org/10.1002/elan.201800204.

Liu, B., Xiao, B., Cui, L., 2015a. Electrochemical analysis of carbaryl in fruit samples on graphene oxide-ionic liquid composite modified electrode. J. Food Compos. Anal. 40, 14–18. https://doi.org/10.1016/j.jfca.2014.12.010.

Liu, L., Zhang, J., Zhao, J., Liu, F., 2012. Mechanical properties of graphene oxides. Nanoscale 4, 5910–5916. https://doi.org/10.1039/c2nr31164j.

Liu, Q., Fei, A., Huan, J., Mao, H., Wang, K., 2015b. Effective amperometric biosensor for carbaryl detection based on covalent immobilization acetylcholinesterase on multiwall carbon nanotubes/graphene oxide nanoribbons nanostructure. J. Electroanal. Chem. 740, 8–13. https://doi.org/10.1016/j.jelechem.2014.12.037.

Liu, T., Su, H., Qu, X., Ju, P., Cui, L., Ai, S., 2011. Acetylcholinesterase biosensor based on 3-carboxyphenylboronic acid/reduced graphene oxide-gold nanocomposites modified electrode for amperometric detection of organophosphorus and carbamate pesticides. Sensor. Actuator. B Chem. 160, 1255–1261. https://doi.org/10.1016/j.snb.2011.09.059.

Liu, Y., Wang, G., Li, C., Zhou, Q., Wang, M., Yang, L., 2014. A novel acetylcholinesterase biosensor based on carboxylic graphene coated with silver nanoparticles for pesticide detection. Mater. Sci. Eng. C 35, 253–258. https://doi.org/10.1016/j.msec.2013.10.036.

Luo, R., Feng, Z., Shen, G., Xiu, Y., Zhou, Y., Niu, X., Wang, H., 2018. Acetylcholinesterase biosensor based on mesoporous hollow carbon spheres/core-shell magnetic nanoparticles-modified electrode for the detection of organophosphorus pesticides. Sensors 18. https://doi.org/10.3390/s18124429.

Mahmood, A., Malik, R.N., 2014. Human health risk assessment of heavy metals via consumption of contaminated vegetables collected from different irrigation sources in Lahore, Pakistan. Arab. J. Chem. 7, 91–99. https://doi.org/10.1016/J.ARABJC.2013.07.002.

Mahmoudi, E., Fakhri, H., Hajian, A., Afkhami, A., Bagheri, H., 2019. High-performance electrochemical enzyme sensor for organophosphate pesticide detection using modified metal-organic framework sensing platforms. Bioelectrochemistry 130, 107348. https://doi.org/10.1016/j.bioelechem.2019.107348.

Mahmoudpour, M., Saadati, A., Hasanzadeh, M., Kholafazad-kordasht, H., 2021. A stretchable glove sensor toward rapid monitoring of trifluralin: a new platform for the on-site recognition of herbicides based on wearable flexible sensor technology using lab-on-glove. J. Mol. Recogn. 34 https://doi.org/10.1002/jmr.2923.

Malard, L.M., Pimenta, M.A., Dresselhaus, G., Dresselhaus, M.S., 2009. Raman spectroscopy in graphene. Phys. Rep. 473, 51–87. https://doi.org/10.1016/j.physrep.2009.02.003.

Manavalan, S., Veerakumar, P., Chen, S.-M., Lin, K.-C., 2020. Three-dimensional zinc oxide nanostars anchored on graphene oxide for voltammetric determination of methyl parathion. Microchim. Acta 187, 17. https://doi.org/10.1007/s00604-019-4031-3.

Mariyappan, V., Keerthi, M., Chen, S., 2021. Highly selective electrochemical sensor based on gadolinium sul fi de Rod-embedded RGO for the sensing of carbofuran. J. Agric. Food Chem. 1–10. https://doi.org/10.1021/acs.jafc.0c07522.

Mehta, J., Vinayak, P., Tuteja, S.K., Chhabra, V.A., Bhardwaj, N., Paul, A.K., Kim, K.H., Deep, A., 2016. Graphene modified screen printed immunosensor for highly sensitive detection of parathion. Biosens. Bioelectron. 83, 339–346. https://doi.org/10.1016/j.bios.2016.04.058.

Miao, S.S., Wu, M.S., Ma, L.Y., He, X.J., Yang, H., 2016. Electrochemiluminescence biosensor for determination of organophosphorous pesticides based on bimetallic Pt-Au/multi-walled carbon nanotubes modified electrode. Talanta 158, 142–151. https://doi.org/10.1016/j.talanta.2016.05.030.

Michelle, C.O., Caetano, F.R., Papi, M.A.P., Watanabe, E.Y., Marcolino-Júnior, L.H., Bergamini, M.F., 2020. Chemical wet oxidation of carbon nanotubes for electrochemical determination of methyl parathion. J. Anal. Chem. 75, 119–126. https://doi.org/10.1134/S1061934820010128.

Migliorini, F.L., Sanfelice, R.C., Mercante, L.A., Facure, M.H.M., Correa, D.S., 2019. Electrochemical sensor based on polyamide 6/polypyrrole electrospun nanofibers coated with reduced graphene oxide for malathion pesticide detection. Mater. Res. Express 7, 015601. https://doi.org/10.1088/2053-1591/ab5744.

Miyazaki, C.M., Adriano, A.M., Rubira, R.J.G., Constantino, C.J.L., Ferreira, M., 2020. Combining electrochemically reduced graphene oxide and Layer-by-Layer fi lms of

magnetite nanoparticles for carbofuran detection. J. Environ. Chem. Eng. 8, 104294. https://doi.org/10.1016/j.jece.2020.104294.
Mohan, V.B., Jayaraman, K., Bhattacharyya, D., 2020. Brunauer–Emmett–Teller (BET) specific surface area analysis of different graphene materials: a comparison to their structural regularity and electrical properties. Solid State Commun. 320, 114004. https://doi.org/10.1016/j.ssc.2020.114004.
Moraes, F.C., Mascaro, L.H., Machado, S.A.S., Brett, C.M.A., 2009. Direct electrochemical determination of carbaryl using a multi-walled carbon nanotube/cobalt phthalocyanine modified electrode. Talanta 79, 1406–1411. https://doi.org/10.1016/j.talanta.2009.06.013.
Mostofizadeh, A., Li, Y., Song, B., Huang, Y., 2011. Synthesis, properties, and applications of low-dimensional carbon-related nanomaterials. J. Nanomater. 2011 https://doi.org/10.1155/2011/685081.
Nag, A., Mitra, A., Mukhopadhyay, S.C., 2018. Graphene and its sensor-based applications: a review. Sens. Actuator., A Phys. 270, 177–194. https://doi.org/10.1016/j.sna.2017.12.028.
Nagabooshanam, S., John, A.T., Wadhwa, S., Mathur, A., Krishnamurthy, S., Bharadwaj, L.M., 2020. Electro-deposited nano-webbed structures based on polyaniline/multi walled carbon nanotubes for enzymatic detection of organophosphates. Food Chem. 323, 126784. https://doi.org/10.1016/j.foodchem.2020.126784.
Nasrollahzadeh, M., Sajjadi, M., Iravani, S., Varma, R.S., 2021. Carbon-based sustainable nanomaterials for water treatment: state-of-art and future perspectives. Chemosphere 263, 128005. https://doi.org/10.1016/j.chemosphere.2020.128005.
Nehru, R., Hsu, Y.F., Wang, S.F., Dong, C. Di, Govindasamy, M., Habila, M.A., AlMasoud, N., 2021. Graphene oxide@Ce-doped TiO2 nanoparticles as electrocatalyst materials for voltammetric detection of hazardous methyl parathion. Microchim. Acta 188. https://doi.org/10.1007/s00604-021-04847-5.
Noyrod, P., Chailapakul, O., Wonsawat, W., Chuanuwatanakul, S., 2014. The simultaneous determination of isoproturon and carbendazim pesticides by single drop analysis using a graphene-based electrochemical sensor. J. Electroanal. Chem. 719, 54–59. https://doi.org/10.1016/j.jelechem.2014.02.001.
Nunes, G.S., Toscano, I.A., Barceló, D., 1998. Analysis of pesticides in food and environmental samples by enzyme- linked immunosorbent assays. TrAC Trends Anal. Chem. (Reference Ed.). https://doi.org/10.1016/S0165-9936(97)00116-7.
Oliveira, A.C.M., Araújo, D.A.G., Pradela-Filho, L.A., Takeuchi, R.M., Santos, A.L., 2021. A robust and versatile micropipette tip-based miniaturized electrochemical cell for determination of carbendazim. Sensor. Actuator. B Chem. 327 https://doi.org/10.1016/j.snb.2020.128880.
Pedrero, M., Campuzano, S., Pingarrón, J.M., 2017. Quantum dots as components of electrochemical sensing platforms for the detection of environmental and food pollutants: a review. J. AOAC Int. 100, 950–961. https://doi.org/10.5740/JAOACINT.17-0169.
Peng, S., Yang, S., Zhang, X., Jia, J., Chen, Q., Lian, Y., Wang, A., Zeng, B., Yang, H., Li, J., Dan, J., Liao, J., Zhou, S., 2021. Analysis of imidacloprid residues in mango, cowpea and water samples based on portable molecular imprinting sensors. PLoS One 16, e0257042. https://doi.org/10.1371/journal.pone.0257042.
Peres, N.M.R., Guinea, F., Castro Neto, A.H., 2006. Electronic properties of disordered two-dimensional carbon. Phys. Rev. B Condens. Matter 73, 1–23. https://doi.org/10.1103/PhysRevB.73.125411.
Pérez-Fernández, B., Costa-García, A., De La Escosura- Muñiz, A., 2020. Electrochemical (bio)sensors for pesticides detection using screen-printed electrodes. Biosensors 10. https://doi.org/10.3390/bios10040032.
Pop, A., Manea, F., Flueras, A., Schoonman, J., 2017. Simultaneous voltammetric detection of carbaryl and paraquat pesticides on graphene-modified boron-doped diamond electrode. Sensors 17, 1–11. https://doi.org/10.3390/s17092033.
Prasad, B.B., Jauhari, D., Tiwari, M.P., 2014. Doubly imprinted polymer nanofilm-modified electrochemical sensor for ultra-trace simultaneous analysis of glyphosate and glufosinate. Biosens. Bioelectron. 59, 81–88. https://doi.org/10.1016/j.bios.2014.03.019.
Rahemi, V., Vandamme, J.J., Garrido, J.M.P.J., Borges, F., Brett, C.M.A., Garrido, E.M.P. J., 2012. Enhanced host-guest electrochemical recognition of herbicide MCPA using a β-cyclodextrin carbon nanotube sensor. Talanta 99, 288–293. https://doi.org/10.1016/j.talanta.2012.05.053.
Rajakumaran, R., Musuvadhi Babulal, S., Ming Chen, S., Sukanya, R., Karthik, R., Muhammed Shafi, P., Shim, J.-J., Yo-Shiuan, C., 2021. Ingenious design of iron vanadate engulfed 3D porous reduced graphene oxide nanocomposites as a reliable electrocatalyst for the selective amperometric determination of furaltadone in aquatic environments. Appl. Surf. Sci. 569, 151046. https://doi.org/10.1016/j.apsusc.2021.151046.
Ramanathan, S., Thamilselvan, A., Radhika, N., Padmanabhan, D., Durairaj, A., Obadiah, A., Sharmila Lydia, I., Vasanthkumar, S., 2021. Development of rutin-rGO/TiO2 nanocomposite for electrochemical detection and photocatalytic removal of 2,4-DCP. J. Iran. Chem. Soc. 18, 2457–2472. https://doi.org/10.1007/s13738-021-02205-z.
Rana, S., Kaur, R., Jain, R., Prabhakar, N., 2019. Ionic liquid assisted growth of poly(3,4-ethylenedioxythiophene)/reduced graphene oxide based electrode: an improved electro-catalytic performance for the detection of organophosphorus pesticides in beverages. Arab. J. Chem. 12, 1121–1133. https://doi.org/10.1016/j.arabjc.2018.08.008.
Sant, V.S., Carvalho, S.W.M.M., Gevaerd, A., Silva, J.O.S., Santos, E., Carregosa, I.S.C., Wisniewski, A., Marcolino-junior, L.H., Bergamini, F., Midori, E., Pesquisa, G. De, Petr, E., 2020. Electrochemical Sensor Based on Biochar and Reduced Graphene Oxide Nanocomposite for Carbendazim Determination, vol. 220, p. 121334. https://doi.org/10.1016/j.talanta.2020.121334.
Saqib, M., Dorozhko, E.V., Barek, J., Vyskocil, V., Korotkova, E.I., Shabalina, A.V., 2021. A laser reduced graphene oxide grid electrode for the voltammetric determination of carbaryl. Molecules 26, 5050. https://doi.org/10.3390/molecules26165050.
Şenocak, A., Tümay, S.O., Makhseed, S., Demirbas, E., Durmuş, M., 2021. A synergetic and sensitive physostigmine pesticide sensor using copper complex of 3D zinc (II) phthalocyanine-SWCNT hybrid material. Biosens. Bioelectron. 174 https://doi.org/10.1016/j.bios.2020.112819.
Silva, R. de O., da Silva, É.A., Fiorucci, A.R., Ferreira, V.S., 2019. Electrochemically activated multi-walled carbon nanotubes modified screen-printed electrode for voltammetric determination of sulfentrazone. J. Electroanal. Chem. 835, 220–226. https://doi.org/10.1016/j.jelechem.2019.01.018.
Singh, A.P., Balayan, S., Hooda, V., Sarin, R.K., Chauhan, N., 2020. Nano-interface driven electrochemical sensor for pesticides detection based on the acetylcholinesterase enzyme inhibition. Int. J. Biol. Macromol. 164, 3943–3952. https://doi.org/10.1016/j.ijbiomac.2020.08.215.
Soltani-Sarvestani, M., Shamspur, T., Mostafavi, A., Falahati-Pour, S.K., Mohamadi, M., Saljooqi, A., 2020. A novel preconcentration/extraction method for fenitrothion residues and its electrochemical sensing in pistachio kernels. J. Mater. Sci. Mater. Electron. 31, 11268–11275. https://doi.org/10.1007/s10854-020-03675-2.
Song, D., Wang, Y., Lu, X., Gao, Y., Li, Y., Gao, F., 2018. Ag nanoparticles-decorated nitrogen-fluorine co-doped monolayer MoS2 nanosheet for highly sensitive electrochemical sensing of organophosphorus pesticides. Sensor. Actuator. B Chem. 267, 5–13. https://doi.org/10.1016/j.snb.2018.04.016.
Stoytcheva, M., Zlatev, R., Montero, G., Velkova, Z., Gochev, V., 2018. A nanotechnological approach to biosensors sensitivity improvement: application to organophosphorus pesticides determination. Biotechnol. Biotechnol. Equip. 32, 213–220. https://doi.org/10.1080/13102818.2017.1389618.
Sun, X., Gong, Z., Cao, Y., Wang, X., 2013. Acetylcholinesterase biosensor based on poly (diallyldimethylammonium chloride)-multi-walled carbon nanotubes-graphene hybrid film. Nano-Micro Lett. 5, 47–56. https://doi.org/10.3786/nml.v5i1.p47-56.
Tadayon, F., Jahromi, M.N., 2020. A sensitive and selective electrochemical determination of Diazinon based on Au – Pd/rGO – MWCNTs composite : analytical application in water , fruit and vegetable samples. J. Iran. Chem. Soc. 17, 847–857. https://doi.org/10.1007/s13738-019-01819-8.
Tadeo, J.L., 2008. Analysis of Pesticides in Food and Environmental Samples, Analysis of Pesticides in Food and Environmental Samples. https://doi.org/10.1201/9781420007756.
Tadeo, J.L., Albero, B., Pérez, R.A., 2019. Pesticides. In: Analysis of Pesticides in Food and Environmental Samples, scond ed. CRC Press, pp. 1–40. https://doi.org/10.1201/9781351047081-1. Boca Raton : Taylor & Francis, a CRC title, part of the Taylor & Francis imprint, a member of the Taylor & Francis Group, the academic division of T&F Informa, plc, 2019.
Tao, T., Zhou, Y., Ma, M., He, H., Gao, N., Cai, Z., Chang, G., He, Y., 2021. Novel graphene electrochemical transistor with ZrO2/rGO nanocomposites functionalized gate electrode for ultrasensitive recognition of methyl parathion. Sensor. Actuator. B Chem. 328, 128936. https://doi.org/10.1016/j.snb.2020.128936.
Thirumalraj, B., Krishnapandi, A., Chen, S.-M., Sudhakaran, M.S., Choe, H., 2020. Rational design and interlayer effect of dysprosium-stannate nanoplatelets incorporated graphene oxide: a versatile and competent electrocatalyst for toxic carbamate pesticide detection in vegetables. ACS Sustain. Chem. Eng. 8, 17882–17892. https://doi.org/10.1021/acssuschemeng.0c07973.
Thompson, L.A., Darwish, W.S., 2019. Environmental chemical contaminants in food: review of a global problem. J. Toxicol. https://doi.org/10.1155/2019/2345283.
Ţucureanu, V., Matei, A., Avram, A.M., 2016. FTIR spectroscopy for carbon family study. Crit. Rev. Anal. Chem. 46, 502–520. https://doi.org/10.1080/10408347.2016.1157013.
Tümay, S.O., Şenocak, A., Sarı, E., Şanko, V., Durmuş, M., Demirbas, E., 2021. A new perspective for electrochemical determination of parathion and chlorantraniliprole pesticides via carbon nanotube-based thiophene-ferrocene appended hybrid nanosensor. Sensor. Actuator. B Chem. 345, 130344. https://doi.org/10.1016/j.snb.2021.130344.
Ulloa, A.M., Glassmaker, N., Oduncu, M.R., Xu, P., Wei, A., Cakmak, M., Stanciu, L., 2021. Roll-to-Roll manufactured sensors for nitroaromatic organophosphorus pesticides detection. ACS Appl. Mater. Interfaces 13, 35961–35971. https://doi.org/10.1021/acsami.1c08700.
Vasseghian, Y., Dragoi, E.N., Almomani, F., Le, V.T., 2022. Graphene-based materials for metronidazole degradation: a comprehensive review. Chemosphere 286, 131727. https://doi.org/10.1016/j.chemosphere.2021.131727.
Wang, B., Li, Y., Hu, H., Shu, W., Yang, L., Zhang, J., 2020a. Acetylcholinesterase electrochemical biosensors with graphene-transition metal carbides nanocomposites modified for detection of organophosphate pesticides. PLoS One. https://doi.org/10.1371/journal.pone.0231981.
Wang, H., Pan, L., Liu, Y., Ye, Y., Yao, S., 2020b. Electrochemical sensing of nitenpyram based on the binary nanohybrid of hydroxylated multiwall carbon nanotubes/single-wall carbon nanohorns. J. Electroanal. Chem. 862, 113955. https://doi.org/10.1016/j.jelechem.2020.113955.
Wang, H., Zhao, G., Chen, D., Wang, Z., Liu, G., 2016. A sensitive acetylcholinesterase biosensor based on screen printed electrode modified with Fe3O4 nanoparticle and graphene for chlorpyrifos determination. Int. J. Electrochem. Sci. 11, 10906–10918. https://doi.org/10.20964/2016.12.90.
Wang, K., Li, H.N., Wu, J., Ju, C., Yan, J.J., Liu, Q., Qiu, B., 2011a. TiO2-decorated graphene nanohybrids for fabricating an amperometric acetylcholinesterase biosensor. Analyst 136, 3349–3354. https://doi.org/10.1039/c1an15227k.
Wang, K., Liu, Q., Dai, L., Yan, J., Ju, C., Qiu, B., Wu, X., 2011b. A highly sensitive and rapid organophosphate biosensor based on enhancement of CdS-decorated graphene

nanocomposite. Anal. Chim. Acta 695, 84–88. https://doi.org/10.1016/j.aca.2011.03.042.
Wang, L., Li, X., Yang, R., Li, J.-J., Qu, L.-B., 2020c. A highly sensitive and selective electrochemical sensor for pentachlorophenol based on reduced graphite oxide-silver nanocomposites. Food Anal. Methods 13, 2050–2058. https://doi.org/10.1007/s12161-020-01823-2.
Wang, L., Liu, Y., Chen, Y., 2021a. Effective electrochemical sensor based on Au nanoparticles decorated carboxylated multi-wall carbon nanotube (AuNPS@c-MWCNTs) nanocomposites for determination of dicapthon pesticide in agricultural food. Int. J. Electrochem. Sci. 16, 1–13. https://doi.org/10.20964/2021.04.64.
Wang, R., Wang, Y., Qu, H., Zheng, L., 2021b. An acetylcholinesterase-functionalized biosensor for sensitive detection of organophosphorus pesticides based on solution-gated graphene transistors. ACS Agric. Sci. Technol. 1, 372–378. https://doi.org/10.1021/acsagscitech.1c00092.
Wang, Shiru, Wang, Sui, Guo, Z., 2014. Electrochemiluminescence sensor for selective preconcentration and sensitive detection of napropamide using water-soluble sulfonated graphene. Electroanalysis 26, 849–855. https://doi.org/10.1002/elan.201300629.
Wang, Y., Zhang, S., Du, D., Shao, Y., Li, Z., Wang, J., Engelhard, M.H., Li, J., Lin, Y., 2011c. Self assembly of acetylcholinesterase on a gold nanoparticles-graphene nanosheet hybrid for organophosphate pesticide detection using polyelectrolyte as a linker. J. Mater. Chem. 21, 5319–5325. https://doi.org/10.1039/c0jm03441j.
Whitener, K.E., Sheehan, P.E., 2014. Graphene synthesis. Diam. Relat. Mater. 46, 25–34. https://doi.org/10.1016/j.diamond.2014.04.006.
Wu, L., Lei, W., Han, Z., Zhang, Y., Xia, M., Hao, Q., 2015. A novel non-enzyme amperometric platform based on poly(3-methylthiophene)/nitrogen doped graphene modified electrode for determination of trace amounts of pesticide phoxim. Sensor. Actuator. B Chem. 206, 495–501. https://doi.org/10.1016/j.snb.2014.09.098.
Wu, S., Huang, F., Lan, X., Wang, X., Wang, J., Meng, C., 2013. Electrochemically reduced graphene oxide and Nafion nanocomposite for ultralow potential detection of organophosphate pesticide. Sensor. Actuator. B Chem. 177, 724–729. https://doi.org/10.1016/j.snb.2012.11.069.
Wu, Y.H., Yang, B.J., Han, G.C., Zong, B.Y., Ni, H.Q., Luo, P., Chong, T.C., Low, T.S., Shen, Z.X., 2002. Fabrication of a class of nanostructured materials using carbon nanowalls as the templates. Adv. Funct. Mater. 12, 489. https://doi.org/10.1002/1616-3028(20020805)12:8<489::AID-ADFM489>3.0.CO;2-X.
Wu, Y.H., Yu, T., Shen, Z.X., 2010. Two-dimensional carbon nanostructures: fundamental properties, synthesis, characterization, and potential applications. J. Appl. Phys. 108 https://doi.org/10.1063/1.3460809.
Xiao, F., Li, H., Yan, X., Yan, L., Zhang, X., Wang, M., Qian, C., Wang, Y., 2020. Graphitic carbon nitride/graphene oxide (g-C3N4/GO) nanocomposites covalently linked with ferrocene containing dendrimer for ultrasensitive detection of pesticide. Anal. Chim. Acta 1103, 84–96. https://doi.org/10.1016/j.aca.2019.12.066.
Xie, X., Zhou, B., Zhang, Y., Zhao, G., Zhao, B., 2021. A multi-residue electrochemical biosensor based on graphene/chitosan/parathion for sensitive organophosphorus pesticides detection. Chem. Phys. Lett. 767, 138355. https://doi.org/10.1016/j.cplett.2021.138355.
Yan, J., Guan, H., Yu, J., Chi, D., 2013. Acetylcholinesterase biosensor based on assembly of multiwall carbon nanotubes onto liposome bioreactors for detection of organophosphates pesticides. Pestic. Biochem. Physiol. 105, 197–202. https://doi.org/10.1016/j.pestbp.2013.02.003.
Yang, S., Luo, S., Liu, C., Wei, W., 2012. Direct synthesis of graphene-chitosan composite and its application as an enzymeless methyl parathion sensor. Colloids Surf. B Biointerfaces 96, 75–79. https://doi.org/10.1016/j.colsurfb.2012.03.007.
Yang, Y., Asiri, A.M., Du, D., Lin, Y., 2014. Acetylcholinesterase biosensor based on a gold nanoparticle-polypyrrole-reduced graphene oxide nanocomposite modified electrode for the amperometric detection of organophosphorus pesticides. Analyst 139, 3055–3060. https://doi.org/10.1039/c4an00068d.
Yao, J., Liu, Z., Jin, M., Zou, Y., Chen, J., Xie, P., Wang, X., Akinoglu, E.M., Zhou, G., Shui, L., 2020. Uniform honeycomb CNT-microparticles prepared via droplet-microfluidics and sacrificial nanoparticles for electrochemical determination of methyl parathion. Sensor. Actuator. B Chem. 321, 128517. https://doi.org/10.1016/j.snb.2020.128517.
Yao, Y., Wang, G., Chu, G., An, X., Guo, Y., Sun, X., 2019. The development of a novel biosensor based on gold nanocages/graphene oxide-chitosan modified acetylcholinesterase for organophosphorus pesticide detection. New J. Chem. 43, 13816–13826. https://doi.org/10.1039/c9nj02556a.
Yao, Y., Zhang, L., Xu, J., Wang, X., Duan, X., Wen, Y., 2014. Rapid and sensitive stripping voltammetric analysis of methyl parathion in vegetable samples at carboxylic acid-functionalized SWCNTs-β-cyclodextrin modified electrode. J. Electroanal. Chem. 713, 1–8. https://doi.org/10.1016/j.jelechem.2013.11.024.
Yi, J., Liu, Z., Liu, J., Liu, H., Xia, F., Tian, D., Zhou, C., 2020. A label-free electrochemical aptasensor based on 3D porous CS/rGO/GCE for acetamiprid residue detection. Biosens. Bioelectron. 148, 111827. https://doi.org/10.1016/j.bios.2019.111827.
Yi, M., Shen, Z., 2015. A review on mechanical exfoliation for the scalable production of graphene. J. Mater. Chem. 3, 11700–11715. https://doi.org/10.1039/c5ta00252d.
Yusuf, M., Kumar, M., Khan, M.A., Sillanpääillanpa, M., Arafat, H., 2019. A review on exfoliation, characterization, environmental and energy applications of graphene and graphene-based composites. Adv. Colloid Interface Sci. 273, 1–23. https://doi.org/10.1016/j.cis.2019.102036.
Zacharia Tano, J., 2011. Identity, physical and chemical properties of pesticides. In: Pesticides in the Modern World - Trends in Pesticides Analysis. InTech. https://doi.org/10.5772/17513.
Zamfir, L.G., Rotariu, L., Bala, C., 2011. A novel, sensitive, reusable and low potential acetylcholinesterase biosensor for chlorpyrifos based on 1-butyl-3-methylimidazolium tetrafluoroborate/multiwalled carbon nanotubes gel. Biosens. Bioelectron. 26, 3692–3695. https://doi.org/10.1016/j.bios.2011.02.001.
Zeng, Y., Zhu, Z., Du, D., Lin, Y., 2016. Nanomaterial-based electrochemical biosensors for food safety. J. Electroanal. Chem. 781, 147–154. https://doi.org/10.1016/j.jelechem.2016.10.030.
Zhai, C., Guo, Y., Sun, X., Zheng, Y., Wang, X., 2014. An acetylcholinesterase biosensor based on graphene-gold nanocomposite and calcined layered double hydroxide. Enzym. Microb. Technol. 58–59, 8–13. https://doi.org/10.1016/j.enzmictec.2014.02.004.
Zhai, C., Sun, X., Zhao, W., Gong, Z., Wang, X., 2013. Acetylcholinesterase biosensor based on chitosan/prussian blue/multiwall carbon nanotubes/hollow gold nanospheres nanocomposite film by one-step electrodeposition. Biosens. Bioelectron. 42, 124–130. https://doi.org/10.1016/j.bios.2012.10.058.
Zhang, C., Zhao, F., She, Y., Hong, S., Cao, X., Zheng, L., Wang, S., Li, T., Wang, M., Jin, M., Jin, F., Shao, H., Wang, J., 2019a. A disposable molecularly imprinted sensor based on Graphe@AuNPs modified screen-printed electrode for highly selective and sensitive detection of cyhexatin in pear samples. Sensor. Actuator. B Chem. 284, 13–22. https://doi.org/10.1016/j.snb.2018.12.075.
Zhang, J., Ji, Y., Wang, R., Zhong, Y., Yan, J., Song, Q., Chenjin Song, Y., Chen, H., 2021. Three-dimensional porous carbon materials from waste of botanical drugs as an efficient biosensing platform for pesticides sensing. Int. J. Electrochem. Sci. 16, 1–16. https://doi.org/10.20964/2021.02.28.
Zhang, L., Zhang, A., Du, D., Lin, Y., 2012. Biosensor based on Prussian blue nanocubes/reduced graphene oxide nanocomposite for detection of organophosphorus pesticides. Nanoscale 4, 4674–4679. https://doi.org/10.1039/c2nr30976a.
Zhang, P., Sun, T., Rong, S., Zeng, D., Yu, H., Zhang, Z., Chang, D., Pan, H., 2019b. A sensitive amperometric AChE-biosensor for organophosphate pesticides detection based on conjugated polymer and Ag-rGO-NH 2 nanocomposite. Bioelectrochemistry 127, 163–170. https://doi.org/10.1016/j.bioelechem.2019.02.003.
Zhang, Y., Liu, H., Yang, Z., Ji, S., Wang, J., Pang, P., Feng, L., Wang, H., Wu, Z., Yang, W., 2015. An acetylcholinesterase inhibition biosensor based on a reduced graphene oxide/silver nanocluster/chitosan nanocomposite for detection of organophosphorus pesticides. Anal. Methods 7, 6213–6219. https://doi.org/10.1039/c5ay01439e.
Zhang, Z., Schniepp, H.C., Adamson, D.H., 2019c. Characterization of graphene oxide: variations in reported approaches. Carbon N. Y. 154, 510–521. https://doi.org/10.1016/j.carbon.2019.07.103.
Zhao, G., Zhou, B., Wang, X., Shen, J., Zhao, B., 2021. Detection of organophosphorus pesticides by nanogold/mercaptomethamidophos multi-residue electrochemical biosensor. Food Chem. 354 https://doi.org/10.1016/j.foodchem.2021.129511.
Zhao, Y., Zheng, X., Wang, Q., Zhe, T., Bai, Y., Bu, T., Zhang, M., Wang, L., 2020. Electrochemical behavior of reduced graphene oxide/cyclodextrins sensors for ultrasensitive detection of imidacloprid in brown rice. Food Chem. 333, 127495. https://doi.org/10.1016/j.foodchem.2020.127495.
Zheng, Y., Liu, Z., Jing, Y., Li, J., Zhan, H., 2015a. An acetylcholinesterase biosensor based on ionic liquid functionalized graphene-gelatin-modified electrode for sensitive detection of pesticides. Sensor. Actuator. B Chem. 210, 389–397. https://doi.org/10.1016/j.snb.2015.01.003.
Zheng, Y., Liu, Z., Zhan, H., Li, J., Zhang, C., 2016. Studies on electrochemical organophosphate pesticide (OP) biosensor design based on ionic liquid functionalized graphene and a Co3O4 nanoparticle modified electrode. Anal. Methods 8, 5288–5295. https://doi.org/10.1039/c6ay01346e.
Zheng, Y., Liu, Z., Zhan, H., Li, J., Zhang, C., 2015b. Development of a sensitive acetylcholinesterase biosensor based on a functionalized graphene-polyvinyl alcohol nanocomposite for organophosphorous pesticide detection. Anal. Methods 7, 9977–9983. https://doi.org/10.1039/c5ay02666k.
Zhou, S., Xu, H., Liu, J., Wei, Y., Ma, X., Han, Z., Chen, H., 2021. Simplified synthesis of N-doped carbon nanotube arrayed mesoporous carbon for electrochemical detection of amitrole. Chem. Phys. 542, 111074. https://doi.org/10.1016/j.chemphys.2020.111074.
Zhu, W., Liu, W., Li, T., Yue, X., Liu, T., Zhang, W., Yu, S., Zhang, D., Wang, J., 2014. Facile green synthesis of graphene-Au nanorod nanoassembly for on-line extraction and sensitive stripping analysis of methyl parathion. Electrochim. Acta 146, 419–428. https://doi.org/10.1016/j.electacta.2014.09.085.
Zuo, Y., Wang, X., Fan, L., Han, Y., Zhang, G., Guo, Y., 2020. The fabrication of an electrochemical sensing interface based on Pt nanoparticles/MoS 2/graphene nanocomposite for sensitive detection of binaphthol. Int. J. Environ. Anal. Chem. 1–12. https://doi.org/10.1080/03067319.2020.1790542, 00.